Production of quarkonia and heavy flavor states in ATLAS and CMS

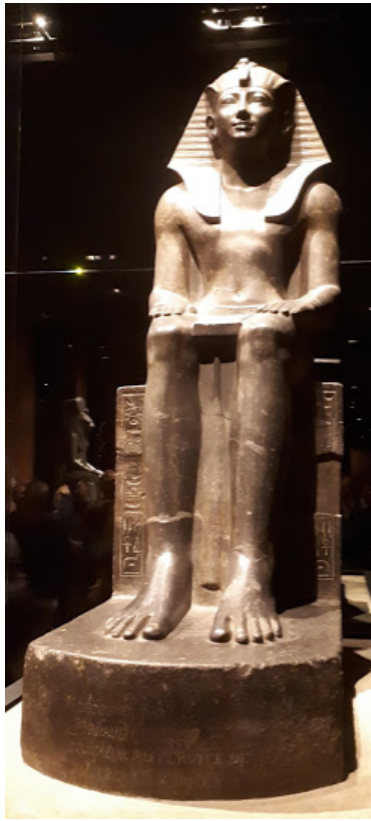

Paolo IENGO
(CERN)
On behalf on the ATLAS and CMS Collaborations

DIS 2019 TORINO
8-12 April
XXVII International Workshop on Deep Inelastic Scattering and Related Subjects

Outline

- Introduction
  - Data sets and general features on Heavy Flavor Physics with ATLAS and CMS
- Quarkonia production
  - J/ψ, ψ(2S), Υ at 5.02 and 8 TeV in pp, pPb, PbPb collisions
  - Associated production of J/ψ and Υ(1S) pairs
- Open Beauty
  - $B^0 \rightarrow K^+\pi^-\mu^+\mu^-$ angular analysis
  - $B^+ \rightarrow K^+\mu^+\mu^-$ angular analysis
  - Search for $X^{\pm}(5568) \rightarrow B^0_s\pi^{\pm}$ resonance
  - B_c^+ ground and excited states
- Observation of $Z \rightarrow J/\psi\, l^+l^-$ decay

Selected recent results among the many published by the two Collaborations

Quarkonia and HF at ATLAS & CMS

- Based on low p_T muon trigger and track reconstruction in the Inner Detector
- Wide rapidity and p_T regions
- Wide $\sqrt{s}$ range: 5.02, 7, 8, 13 TeV
- pp, pA; AA collisions

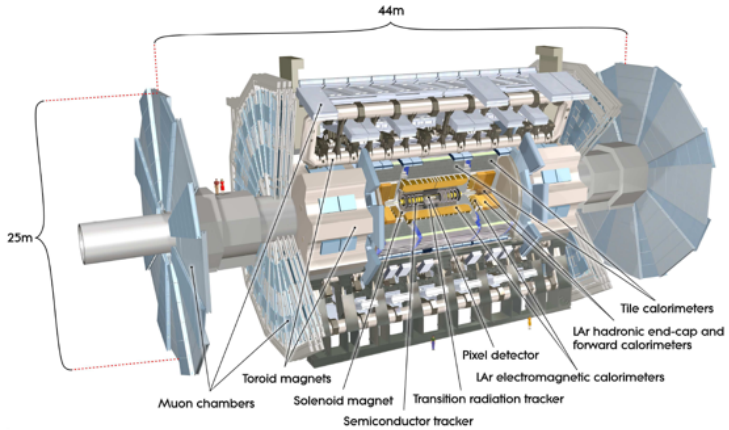

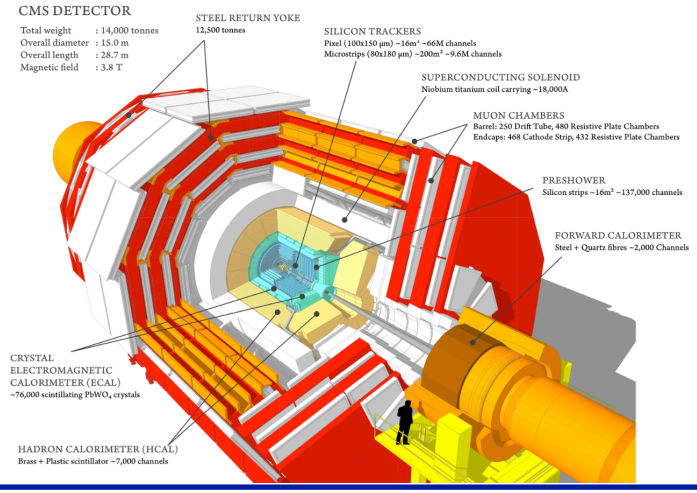

Di-μ invariant mass spectrum

PbPb collision at 5.02 TeV

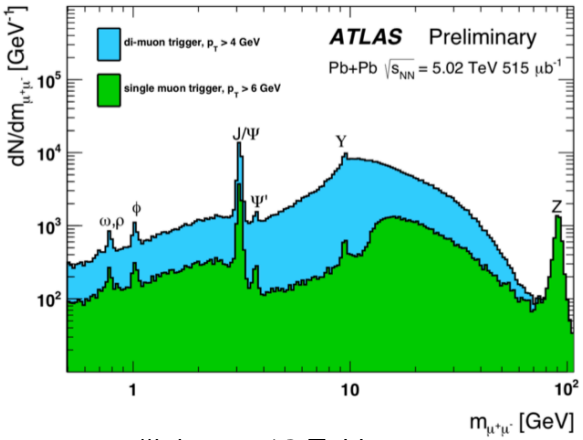

pp collision at 13 TeV

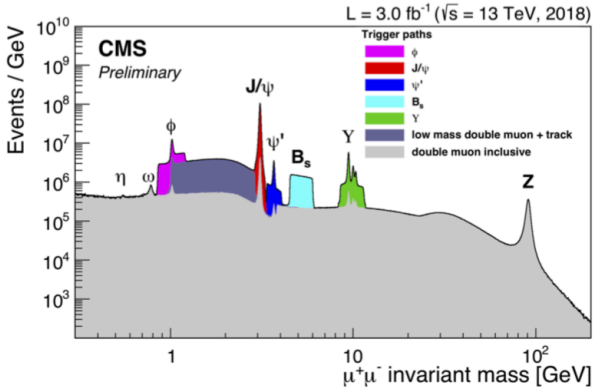

$\Delta p_T/p_T \sim O(1\text{-}5\%)$ for low-momentum tracks

Quarkonia and HF at ATLAS & CMS

- Heavy Flavor production characterized by
  - $M(\mu^+\mu^-)$
  - $\tau(\mu^+\mu^-)$

  } 2D fit
  - Prompt vs Non-Prompt (B decays in flight) production

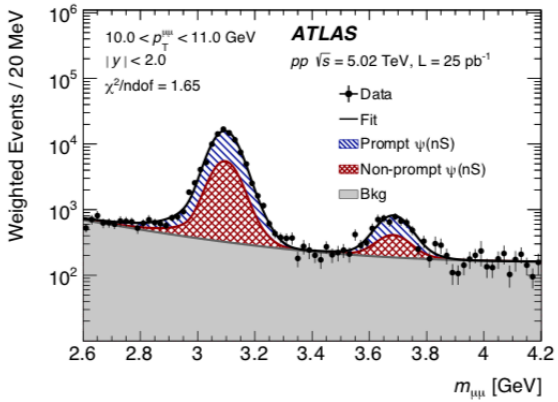

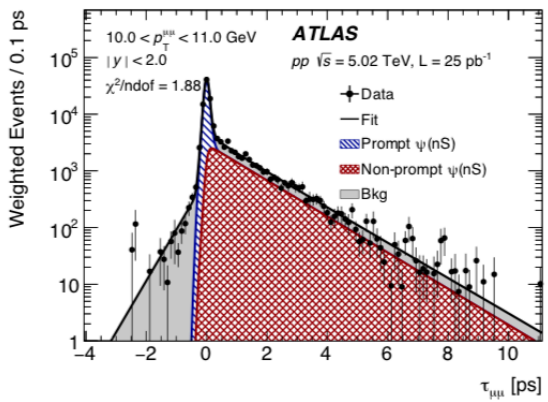

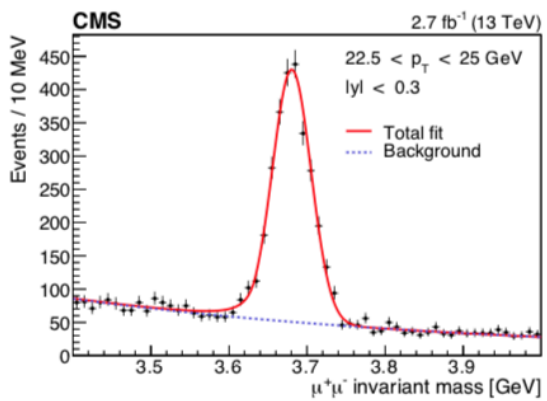

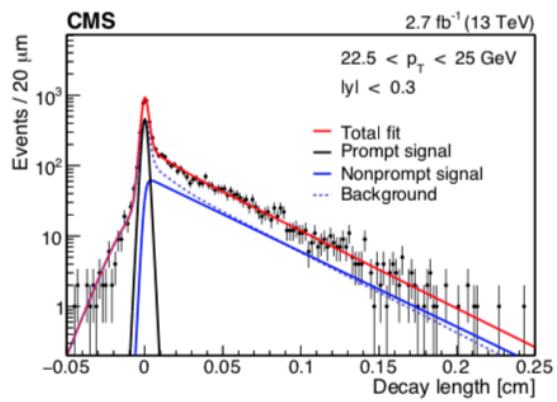

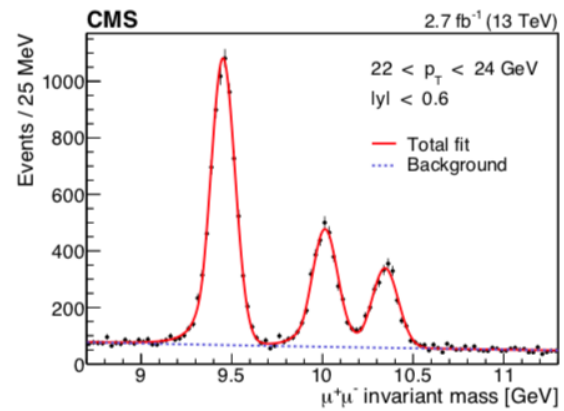

Quarkonia production

- Heavy quarkonium bound states
  - pp collisions: comparison with QCD models, different from prompt and non-prompt production
  - AA collisions: study the deconfined quark-gluon plasma (QGP)
  - pA collision: disentangling the effects from cold nuclear matter (CNM) interactions

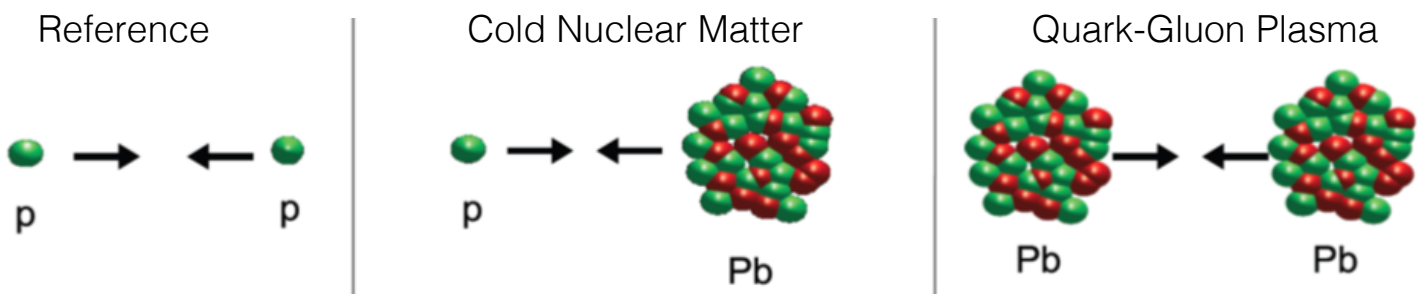

- Observables
  - Differential cross-section
  - Nuclear Modification Factor in pA
  - Nuclear Modification Factor in AA

$$\frac{d^2\sigma_{O(nS)}}{dp_T dy^*} \times B(O(nS) \to \mu^+\mu^-)$$

$$R_{pPb} = \frac{1}{208}\frac{\sigma^{O(nS)}_{p+Pb}}{\sigma^{O(nS)}_{pp}}$$

$$R_{AA} = \frac{N_{AA}}{< T_{AA} > \times \sigma_{pp}}$$

$O(nS) = J/\psi,\ \psi(2S),$ and $\Upsilon(nS)$ $(n = 1, 2, 3)$

$< T_{AA} >$: mean nuclear thickness function

ATLAS: 28 nb^{-1} at 5.02 TeV pPb and 25 pb^{-1} at 5.02 TeV pp
CMS: ~2.5 fb^{-1} at 7 TeV pp

Prompt J/ψ and ψ(2S) in pp

Eur. Phys. J. C 78 (2018) 171

Phys. Lett. B 780 (2018) 251

Prompt J/ψ at 5.02 TeV

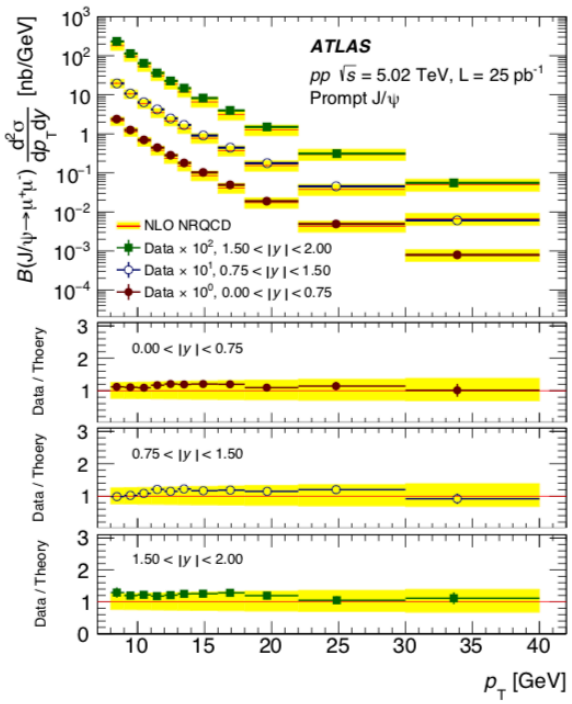

Prompt ψ(2S) at 5.02 TeV

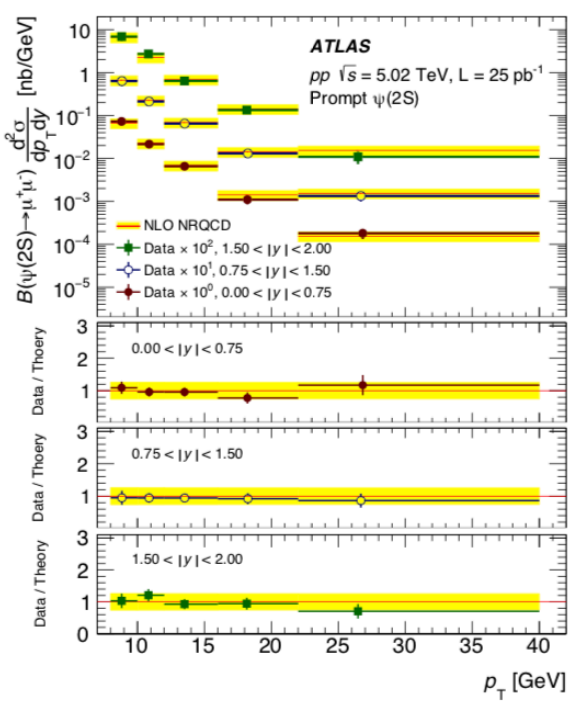

Prompt J/ψ and ψ(2S) at 13 TeV

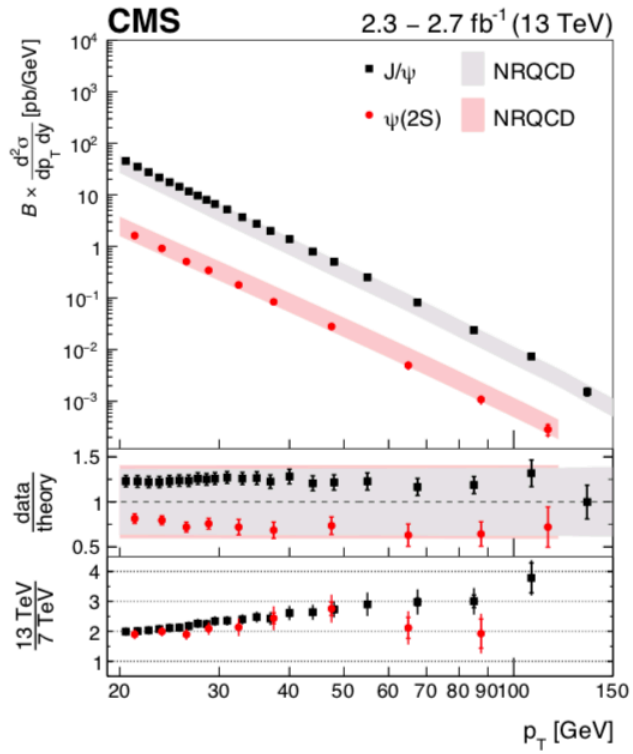

- Good description of the data by NLO NRQCD (prompt) calculations in the full p_T range (same at 7 and 8 TeV)

Non-prompt J/ψ and ψ(2S) in pp

Eur. Phys. J. C 78 (2018) 171

Non-prompt J/ψ at 5.02 TeV

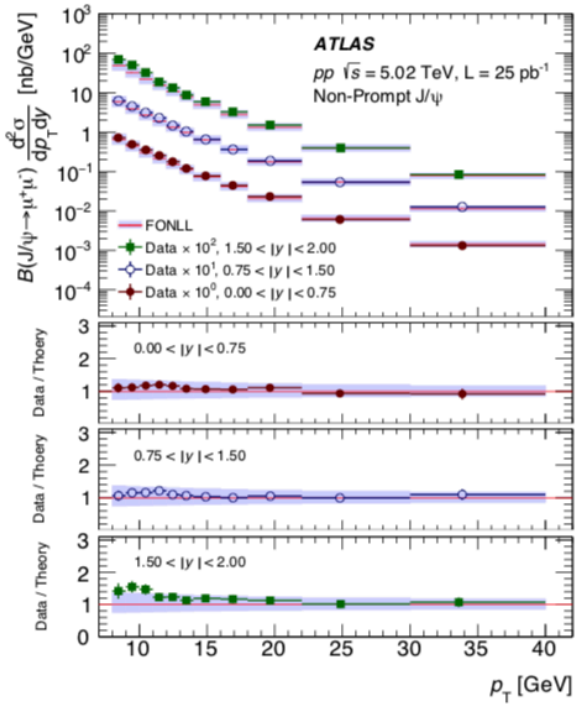

Non-prompt ψ(2S) at 5.02 TeV

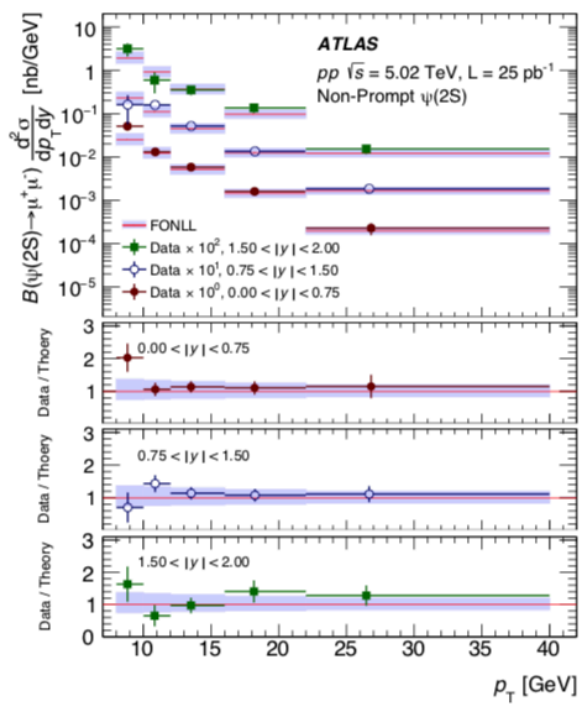

- Good description of the data by FONLL (non-prompt) calculations in the full p_T range

Υ production in pp

Υ production in pp collision at 5.02 TeV

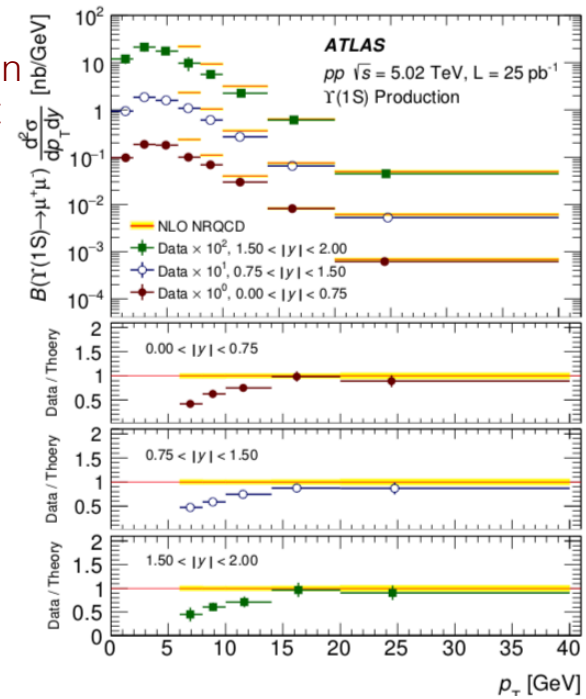

Eur. Phys. J. C 78 (2018) 171

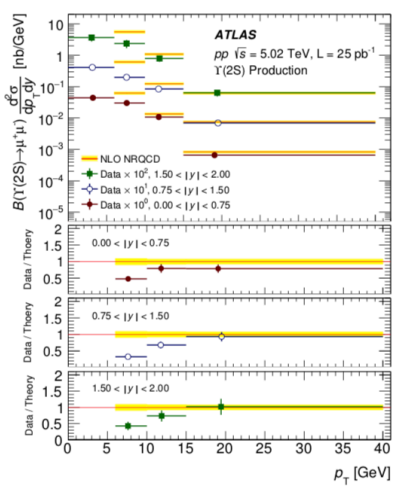

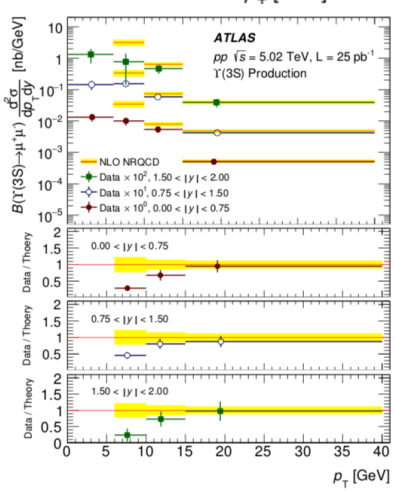

Υ production in pp collision at 13 TeV

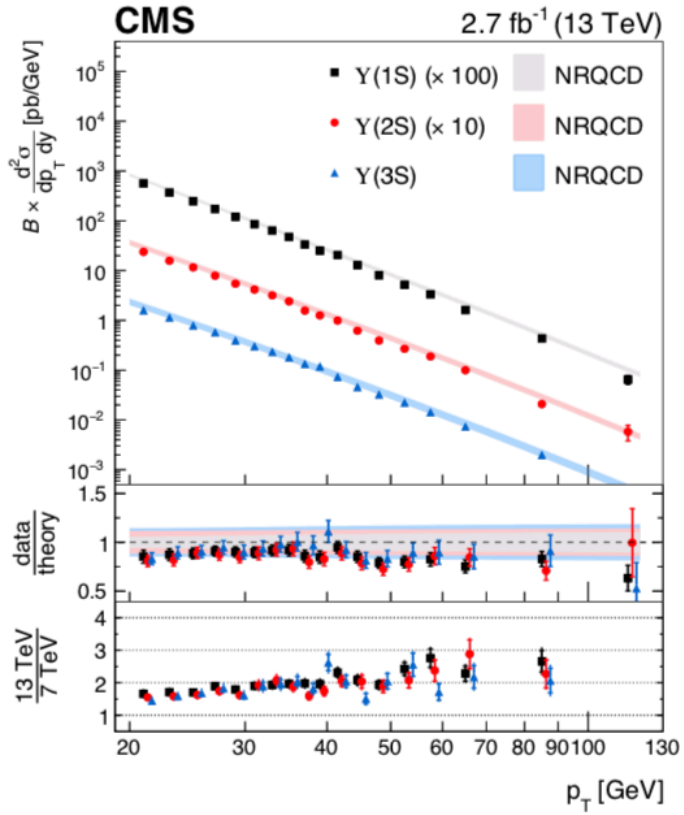

Phys. Lett. B 780 (2018) 251

- Good description of the data by NLO NRQCD for p_T>20 GeV; discrepancies for p_T<15 GeV

J/ψ, ψ(2S) production in pPb 5.02 TeV

Eur. Phys. J. C 78 (2018) 171

Prompt and non-prompt J/ψ

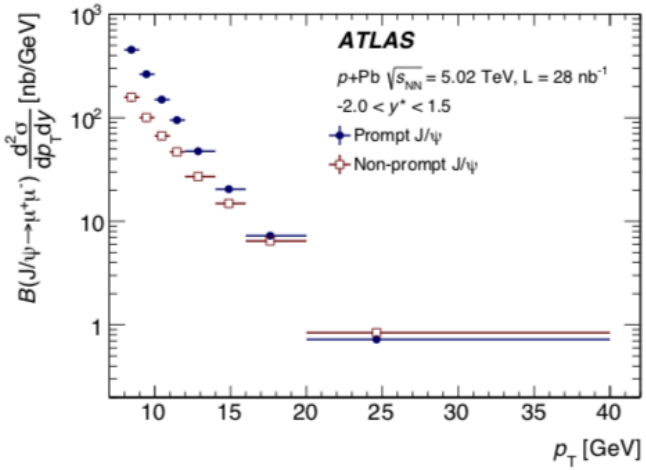

Prompt and non-prompt ψ(2S)

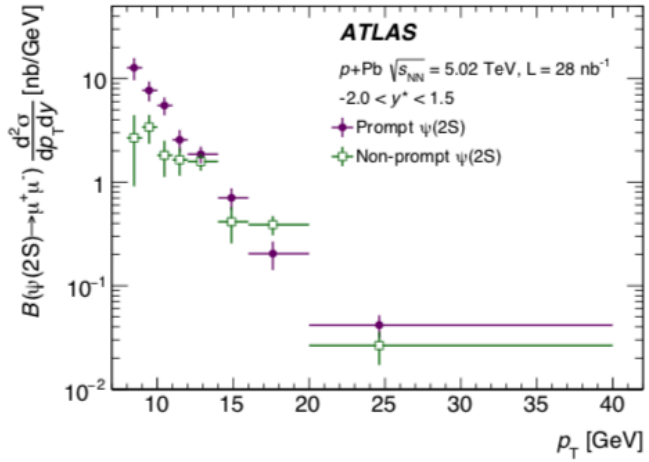

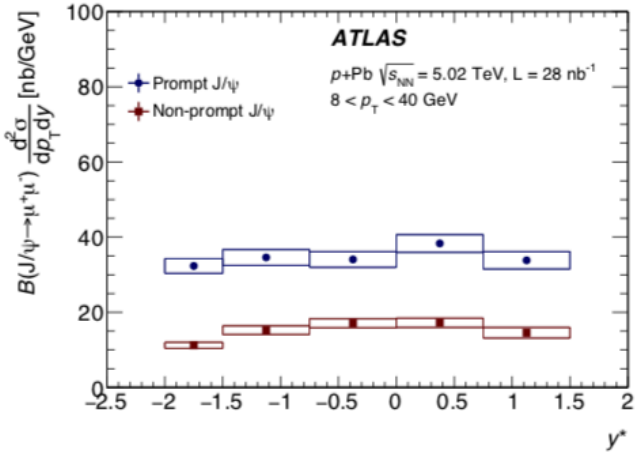

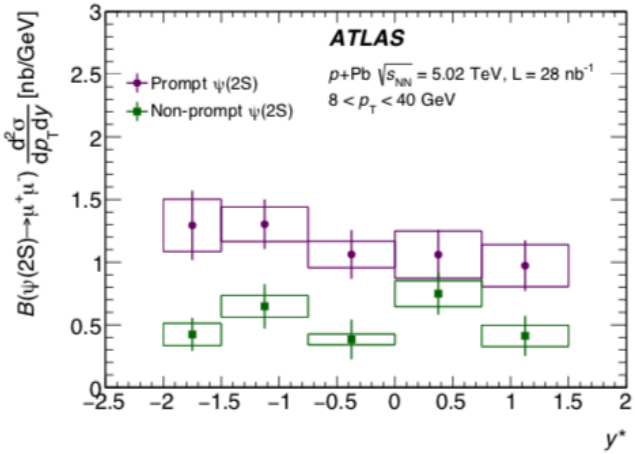

- pPb: improved measurements consistent with previous results

Υ production in pPb at 5.02 TeV

Eur. Phys. J. C 78 (2018) 171

- Difficult to separate Υ(2S) and Υ(3S) at forward and backward y* intervals in pPb collisions → combined

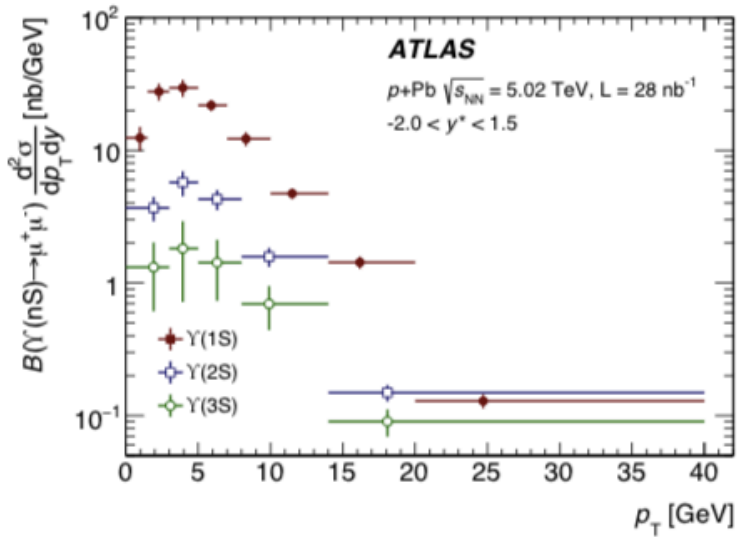

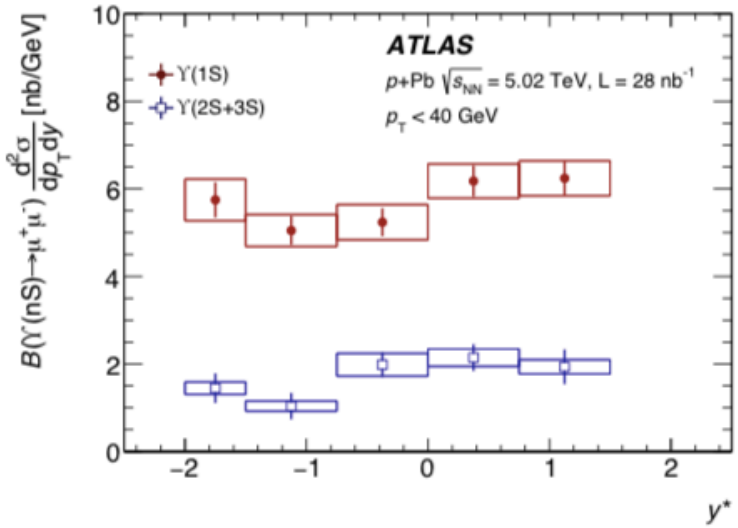

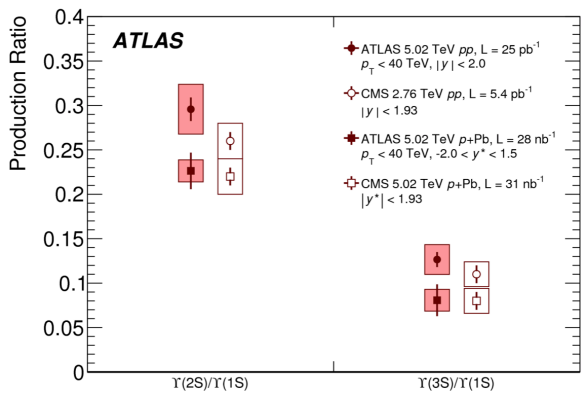

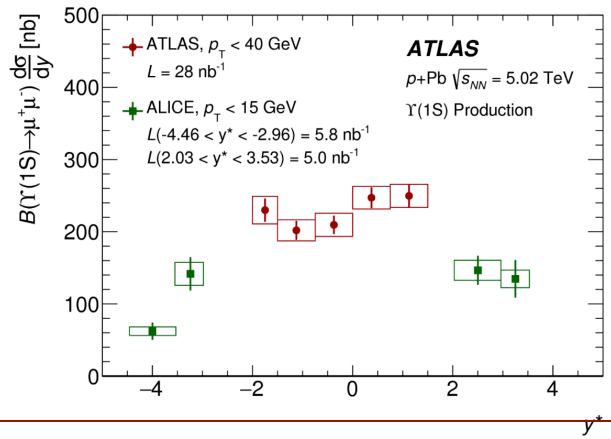

Comparison with CMS: good agreement

Comparison with ALICE: central vs forward

Nuclear Modification Factors: J/ψ and Υ

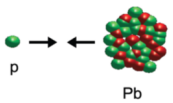

Eur. Phys. J. C 78 (2018) 171

Prompt J/ψ

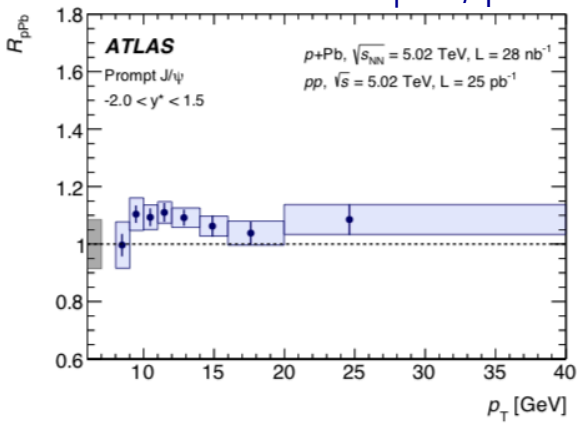

- Non-prompt J/ψ

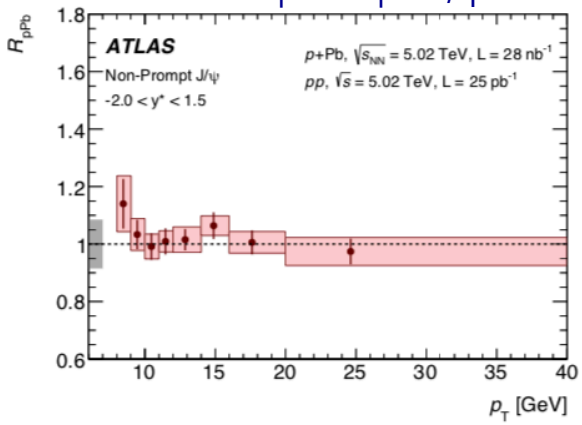

- Υ

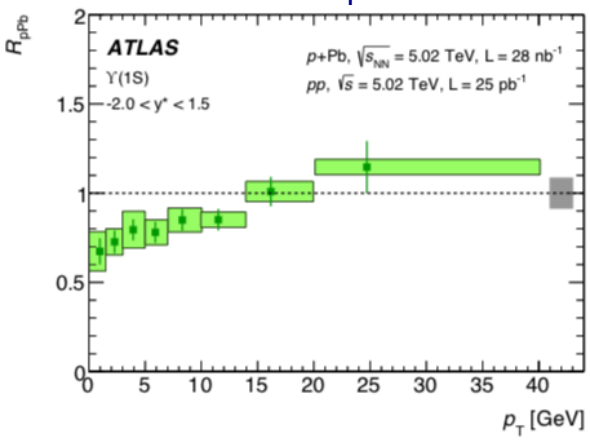

J/ψ: R_{pPb}~1 in the full kinematic range → CNM effects are small for prompt and non-prompt J/ψ production

Υ(1S): Production suppressed at low p_T (<15 GeV) and increases with p_T → CNM effects are relevant for Υ(1S)

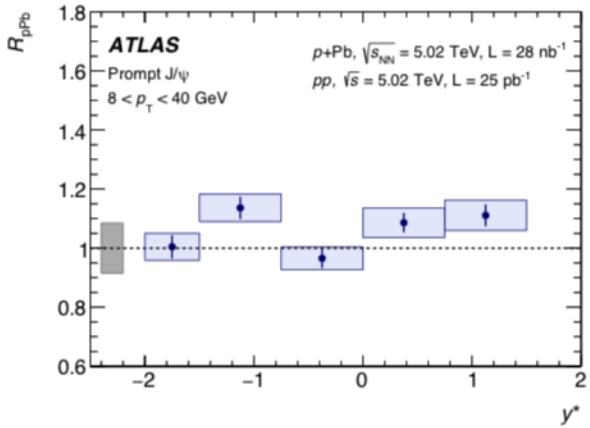

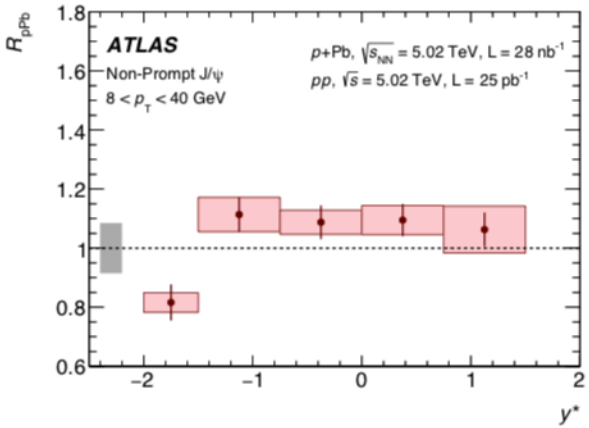

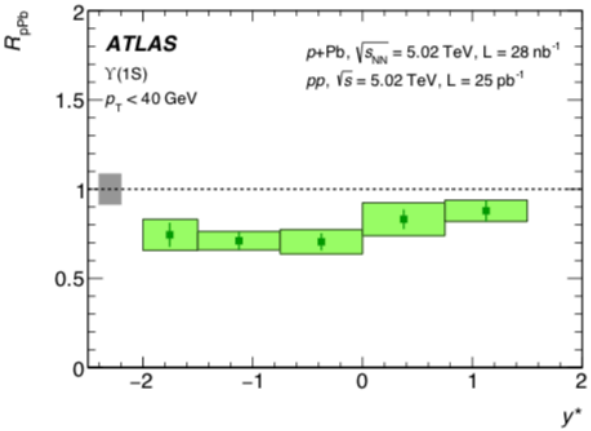

No significant dependency on rapidity observed

Nuclear Modification Factors

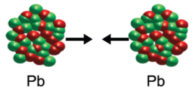

Eur. Phys. J. C 78 (2018) 762

- Comparison between R_{pPb} and R_{PbPb} for prompt and non-prompt J/ψ
  - Very strong suppression of charmonia production in PbPb collisions
  - Similar for prompt and non-prompt J/ψ production

- Prompt J/ψ

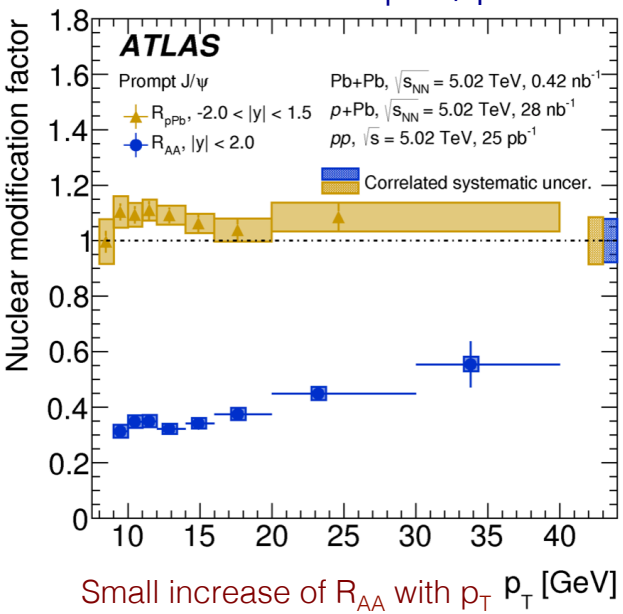

Small increase of R_{AA} with p_T in prompt J/ψ production

- Non-prompt J/ψ

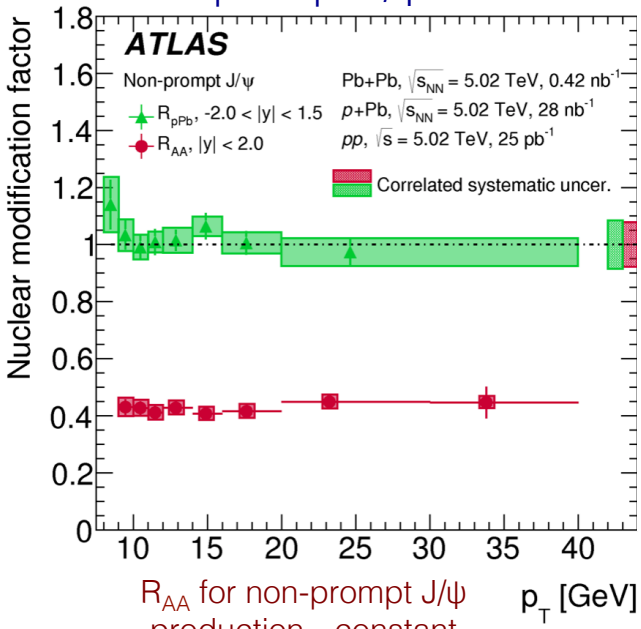

R_{AA} for non-prompt J/ψ production ~constant

- R_{AA} vs N_{jets} in PbPb collisions (Prompt J/ψ)

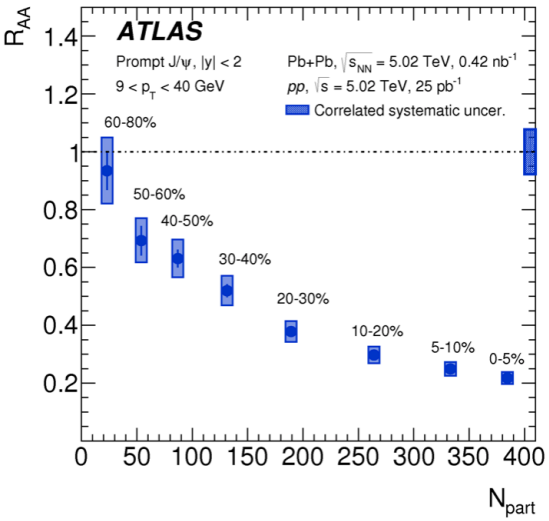

Suppression decreases going from central to peripheral collisions

- Many other interesting measurements and results in PbPb collisions not included here, see e.g.
  - Prompt and non-prompt J/ψ elliptic flow in Pb+Pb collisions at $\sqrt{S_{NN}}$=5.02 TeV with the ATLAS detector (Eur. Phys. J. C 78 (2018) 784)
  - Measurement of suppression and azimuthal anisotropy of muon from heavy-flavor decays in Pb+Pb collisions at $\sqrt{S_{NN}}$=2.76 TeV with the ATLAS detector (Phys. Rev. C 98 (2018) 044905)

Quarkonia associated production

- Associated production of two objects in the same pp collision

  - Single Parton Scattering (SPS)
    - Two quarkonia produced in a single interaction between partons

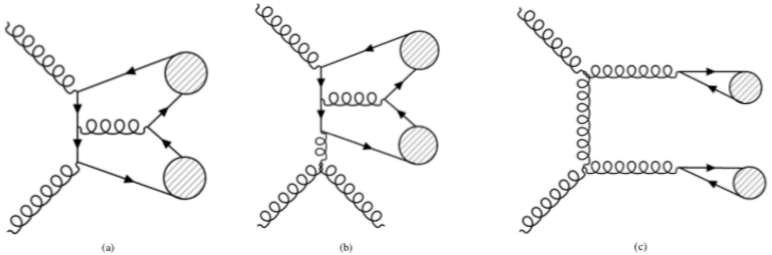

  - Double Parton Scattering (SPS)
    - Simultaneous, independent and uncorrelated interactions of two pairs of partons, each interaction producing a quarkonium
    - Cross-section sensitive to spatial distribution of gluons in the proton

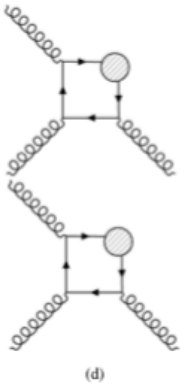

$$\sigma_{\text{eff}} = \frac{1}{2}\frac{\sigma^2_{J/\psi}}{\sigma^{J/\psi,J/\psi}_{\text{DPS}}} = \frac{1}{2}\frac{\sigma^2_{J/\psi}}{f_{\text{DPS}} \times \sigma_{J/\psi J/\psi}}$$

f_{DPS} = fraction of DPS events

σ_{eff} ~(2-20) mb assumed to be independent of the scattering process and $\sqrt{s}$; related to the spatial separation between partons inside the proton

Large uncertainties on DPS due to possible higher-order SPS contributions, feed-down and limited knowledge of the proton's transverse profile

Di-J/ψ production at 8 TeV

Eur. Phys. J. C 77 (2017) 76

ATLAS: 11.4 fb^{-1} at 8 TeV pp

- Two prompt J/ψ → μμ decays from the same pp collision
  - Invariant mass fit
  - Pseudo-proper decay time fits → prompt-prompt
  - Vertex d_Z fit → two J/ψ from the same vertex (pileup-removal)
- Data driven SPS contribution
- Analysis in two regions according to sub-leading J/ψ_2 rapidity

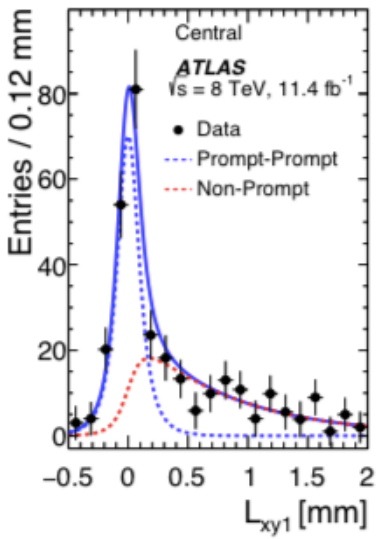

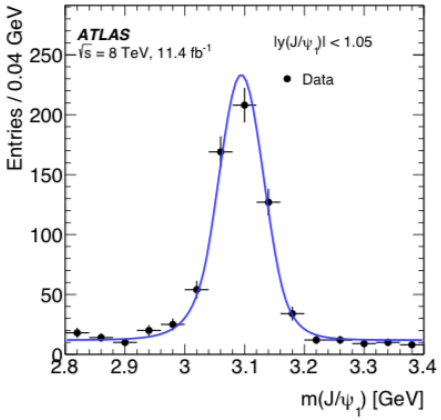

$$|y^*_{J/\psi_2}| < 1.05 \qquad 1.05 < |y^*_{J/\psi_2}| < 2.1$$

$$N_{J/\psi J/\psi} = 3310 \pm 330 \qquad N_{J/\psi J/\psi} = 3140 \pm 370$$

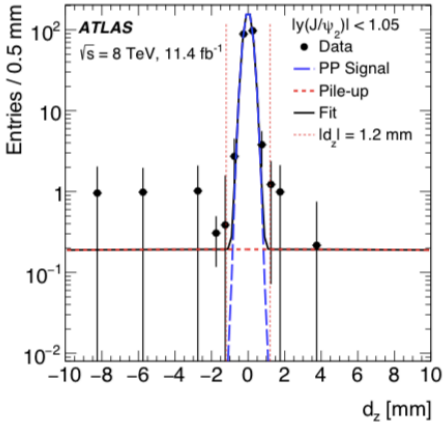

Cross—section in fiducial region

$$\sigma_{\mathrm{Fid}}(pp \to J/\psi J/\psi + X) =$$

$$\begin{cases} 15.6 \pm 1.3\ (\mathrm{stat}) \pm 1.2\ (\mathrm{syst}) \pm 0.2\ (\mathrm{BF}) \pm 0.3\ (\mathrm{lumi})\ \mathrm{pb},\ \text{for } |y| < 1.05, \\ 13.5 \pm 1.3\ (\mathrm{stat}) \pm 1.1\ (\mathrm{syst}) \pm 0.2\ (\mathrm{BF}) \pm 0.3\ (\mathrm{lumi})\ \mathrm{pb},\ \text{for } 1.05 \le |y| < 2.1 \end{cases}$$

$$p_{T\,J/\psi_2} > 8.5\,GeV$$
$$|y^*_{J/\psi_2}| < 2.1$$
$$p_T(\mu) > 2.5\,GeV$$
$$|\eta(\mu)| < 2.3$$

- Extrapolating to the full acceptance (assuming unpolarized J/ψ):

$$\sigma(pp \to J/\psi J/\psi + X) = \begin{cases} 82.2 \pm 8.3\ (\mathrm{stat}) \pm 6.3\ (\mathrm{syst}) \pm 0.9\ (\mathrm{BF}) \pm 1.6\ (\mathrm{lumi})\ \mathrm{pb},\ \text{for } |y| < 1.05, \\ 78.3 \pm 9.2\ (\mathrm{stat}) \pm 6.6\ (\mathrm{syst}) \pm 0.9\ (\mathrm{BF}) \pm 1.5\ (\mathrm{lumi})\ \mathrm{pb},\ \text{for } 1.05 \le |y| < 2.1 \end{cases}$$

Di-J/ψ production at 8 TeV

Eur. Phys. J. C 77 (2017) 76

- DPS vs SPS undistinguishable on event-by-event base
- Different overall kinematics → angular correlation: Δy and Δφ (bin event re-weighting)

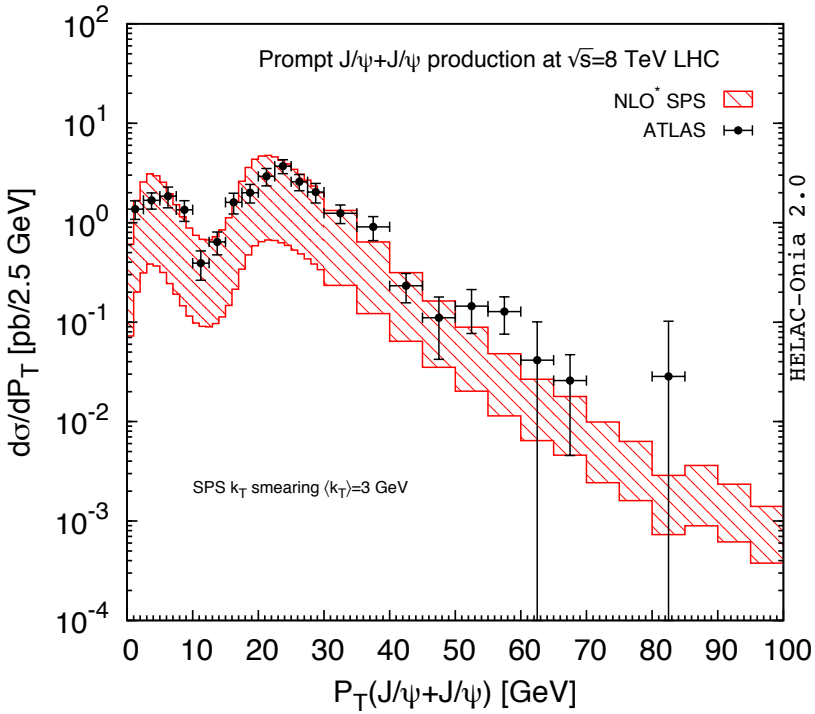

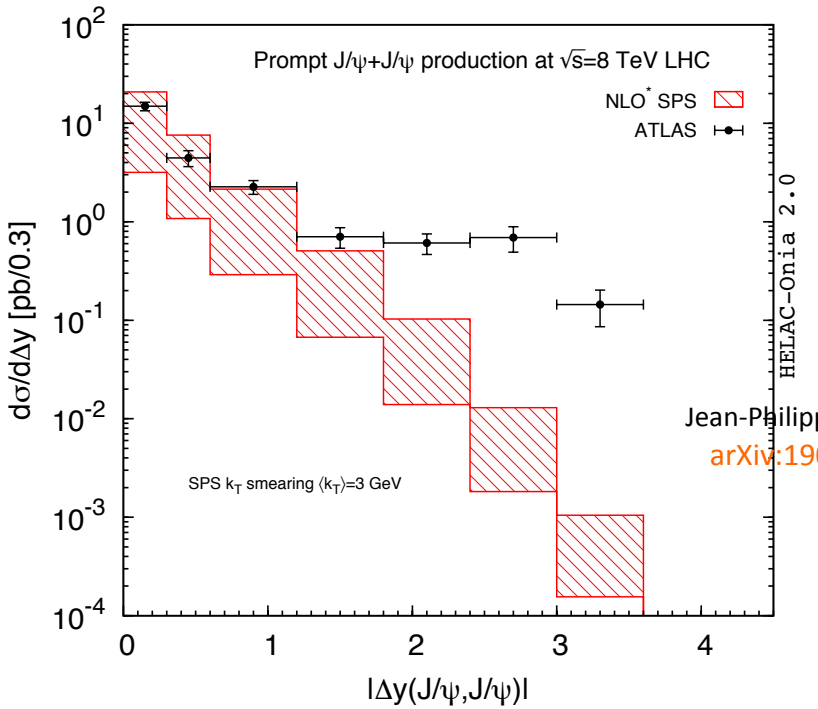

Jean-Philippe Lansberg
arXiv:1903.09185v1

- General agreement with NLO* SPS (with feed-down correction factor) + LO DPS (normalised to measurements)

$$f_{DPS} = (9.2 \pm 2.1\ (\text{stat}) \pm 0.5\ (\text{syst}))\%$$

Effective cross-section of DPS

$$\sigma_{\text{eff}} = 6.3 \pm 1.6\ (\text{stat}) \pm 1.0\ (\text{syst}) \pm 0.1\ (\text{BF}) \pm 0.1\ (\text{lumi})\ \text{mb}$$

Υ(1S) pair production at 8 TeV

JHEP 05 (2017) 013

CMS: 20.7 fb^{-1} at 8 TeV pp

- Υ(1S)Υ(1S) → 4μ decay
- Kinematic fit to oppositely charged muon pair and then on the four muons with common vertex

Fiducial region

$$p_T(\mu) > 2.5 GeV$$
$$|\eta(\mu)| < 2.4$$
$$|y^*_\Upsilon| < 2.0$$

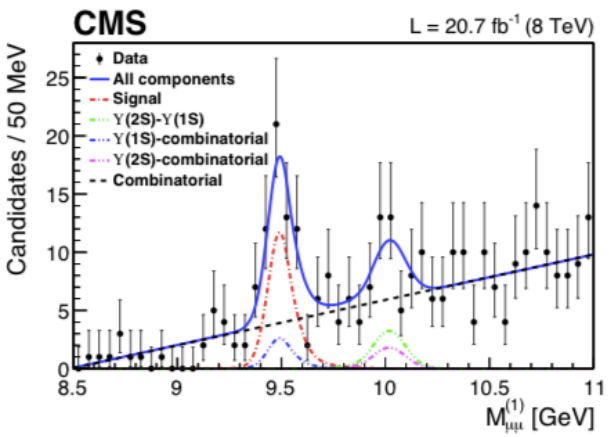

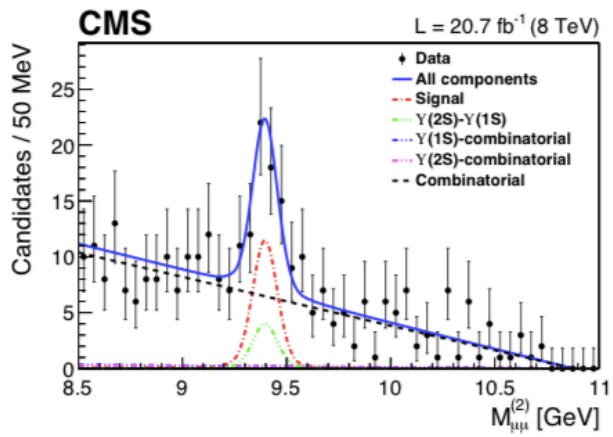

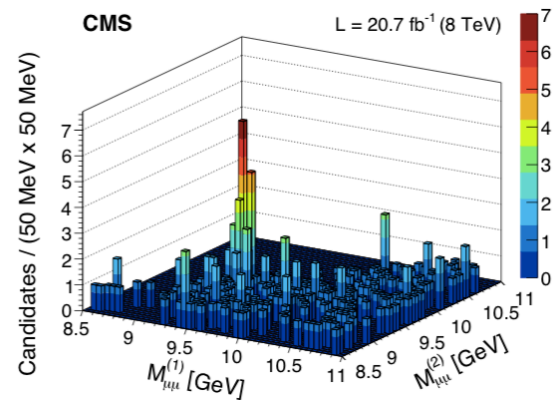

N_{signa}(Υ(1S)Υ(1S)) = 38±7

Very limited statistic!

$$\sigma_{\rm fid} = 68.8 \pm 12.7\,({\rm stat}) \pm 7.4\,({\rm syst}) \pm 2.8\,(\mathcal{B})\,{\rm pb}$$

$$\sigma_{\rm eff} \approx 2.2 - 6.6\ {\rm mb}$$

Assuming both mesons decaying isotropically (polarisation effects: up to ~40% variation)

Quarkonia associated production

- Summary of experimental results (including older ATLAS results on J/ψ associated production with vector bosons)

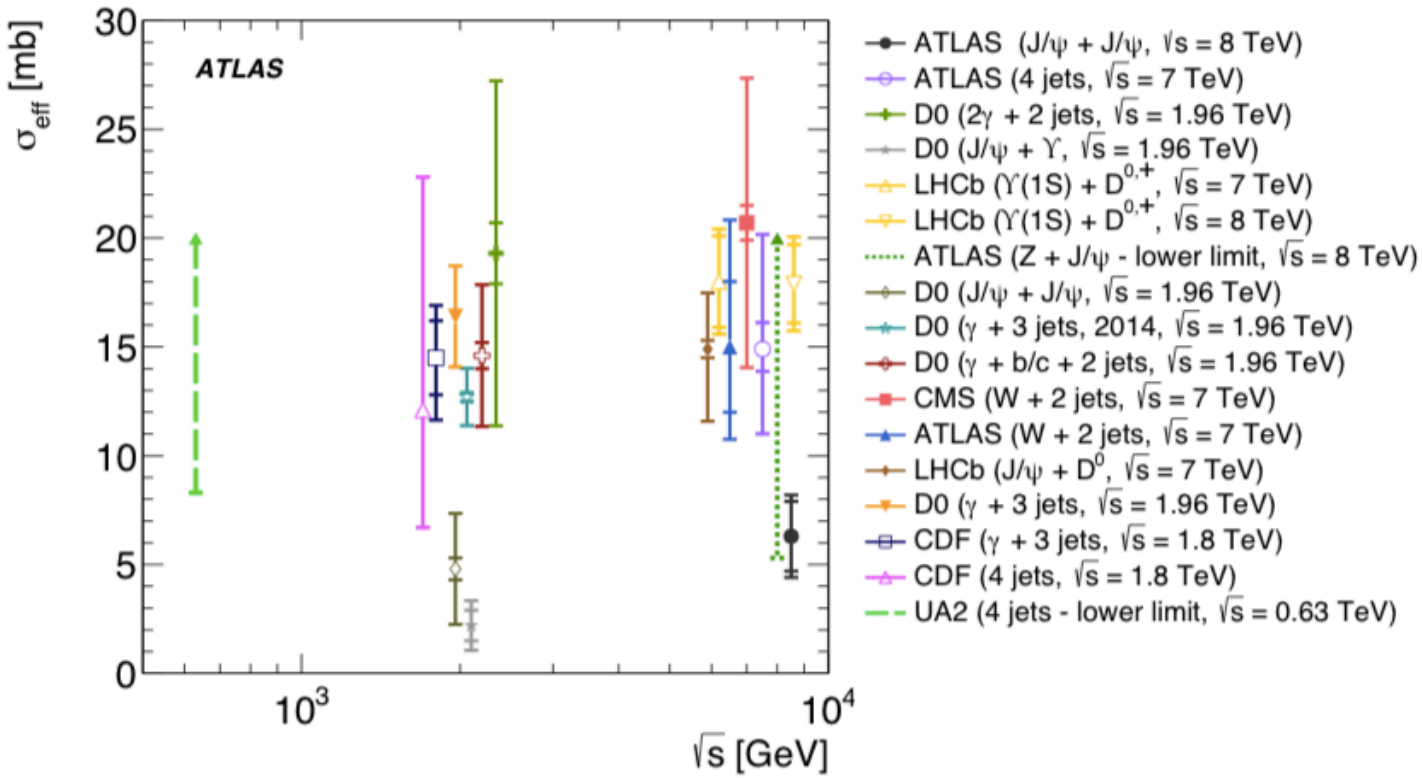

- σ_{eff} generally lower from prompt di-J/ψ and di-ϒ wrt other final states

Quarkonia associated production

- Summary of experimental results (including older ATLAS results on J/ψ associated production with vector bosons)

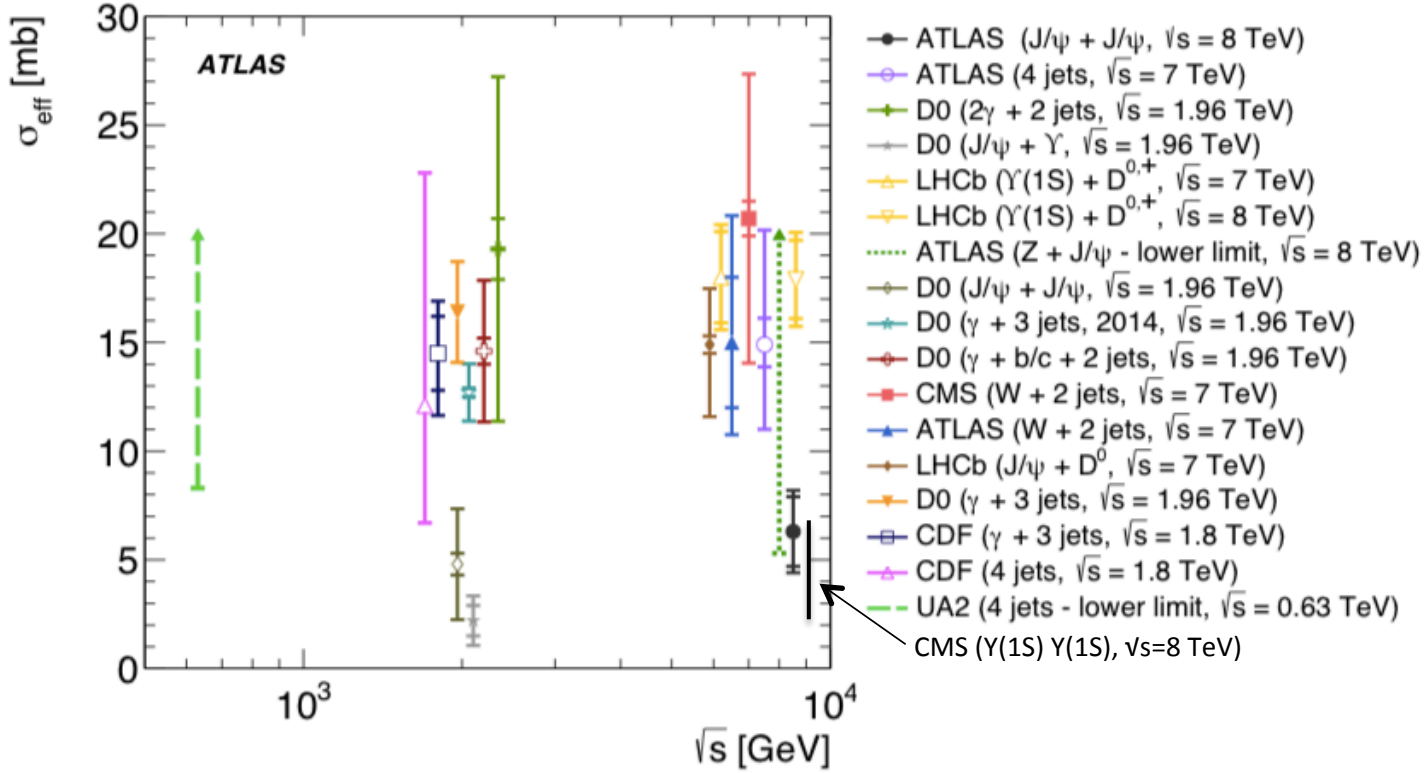

- σ_{eff} generally lower from prompt di-J/ψ and di-ϒ wrt other final states
- Quarkonium final states dominantly produced from gluon-gluon interactions; jet-related channels by quark-antiquark and quark-gluon parton interactions
- Average transverse distance between gluons in the proton smaller than between quarks, or between quarks and gluons?

Heavy Flavor: Open Beauty

$B^0 \rightarrow K^{*0}\mu^+\mu^-$ angular analysis

- $B^0 \rightarrow K^{*0}\mu^+\mu^- \rightarrow K^+\pi^-\mu^+\mu^-$ is a FCNC process
- The process can be fully described by the three angles (θ_L, θ_K, ϕ) and the dimuon invariant mass squared q^2
- New physics entering the loop can be detected by looking at the **angular** distributions of the decay

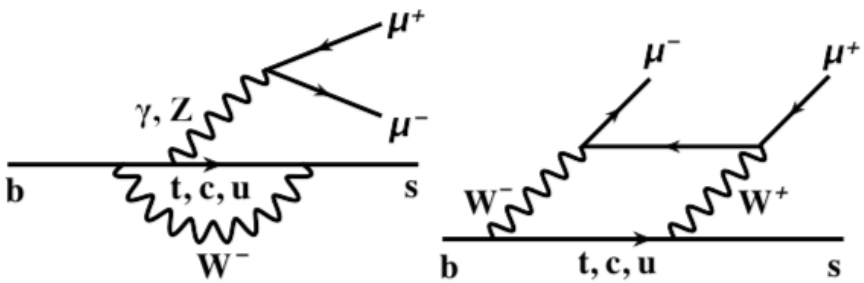

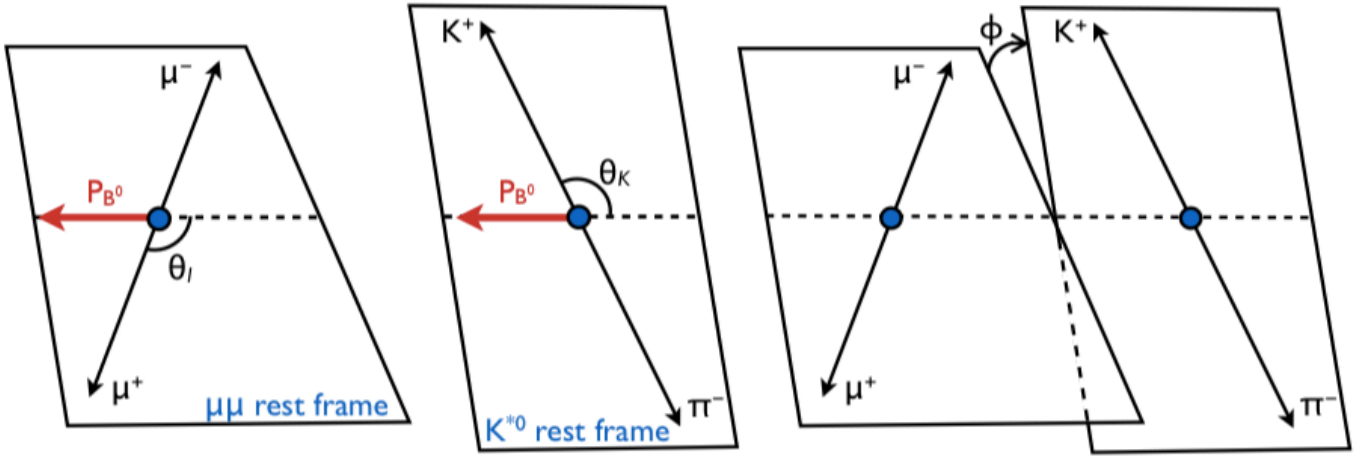

$B^0 \rightarrow K^{*0}\mu^+\mu^-$ angular analysis

- Angular differential decay rate expressed with S coefficients that may be represented by helicity or transversity amplitudes:

$$\frac{1}{d\Gamma/dq^2}\frac{d^4\Gamma}{d\cos\theta_L d\cos\theta_K d\phi dq^2} = \frac{9}{32\pi}\Bigg[\frac{3(1-F_L)}{4}\sin^2\theta_K + F_L\cos^2\theta_K + \frac{1-F_L}{4}\sin^2\theta_K\cos 2\theta_L$$
$$-F_L\cos^2\theta_K\cos 2\theta_L + S_3\sin^2\theta_K\sin^2\theta_L\cos 2\phi$$
$$+S_4\sin 2\theta_K\sin 2\theta_L\cos\phi + S_5\sin 2\theta_K\sin\theta_L\cos\phi$$
$$+S_6\sin^2\theta_K\cos\theta_L + S_7\sin 2\theta_K\sin\theta_L\sin\phi$$
$$+S_8\sin 2\theta_K\sin 2\theta_L\sin\phi + S_9\sin^2\theta_K\sin^2\theta_L\sin 2\phi\Bigg]. \qquad (1)$$

$$A_{FB} = 3S_6/4$$

Forward-backward Asymmetry
F_L = fraction of longitudinally polarised K*
F_S = s-wave fraction

$$P_1 = \frac{2S_3}{1-F_L}$$
$$P_2 = \frac{2}{3}\frac{A_{FB}}{1-F_L}$$
$$P_3 = -\frac{S_9}{1-F_L}$$
$$P'_{j=4,5,6,8} = \frac{S_{i=4,5,7,8}}{\sqrt{F_L(1-F_L)}}.$$

- Generally written in terms of P and P' observables as they are less sensitive to theoretical uncertainties at LO
- LHCb measured a >3σ discrepancy with model on P'_5

ATLAS and CMS analysis uses ~20 fb^{-1} of 8 TeV pp data taken in 2012
ATLAS extracts P_1 and P'_i (i=4,5,6,8); CMS extracts P_1 and P'_5

$B^0 \rightarrow K^{*0}\mu^+\mu^-$ angular analysis

- ATLAS: fit signal and background
  - Four different fits, 3 free parameters each
  - FL, S3 common to each fit
  - S4, S5, S7, S8 fitted parameters
  - P1, Pi' extracted from fit parameters
  - S-wave component (non-resonant Kπ) neglected and included as systematics
  - 340 events in 3 q^2 bins
    - Signal PDF folded to reduce the number of free parameters and improve fit convergence

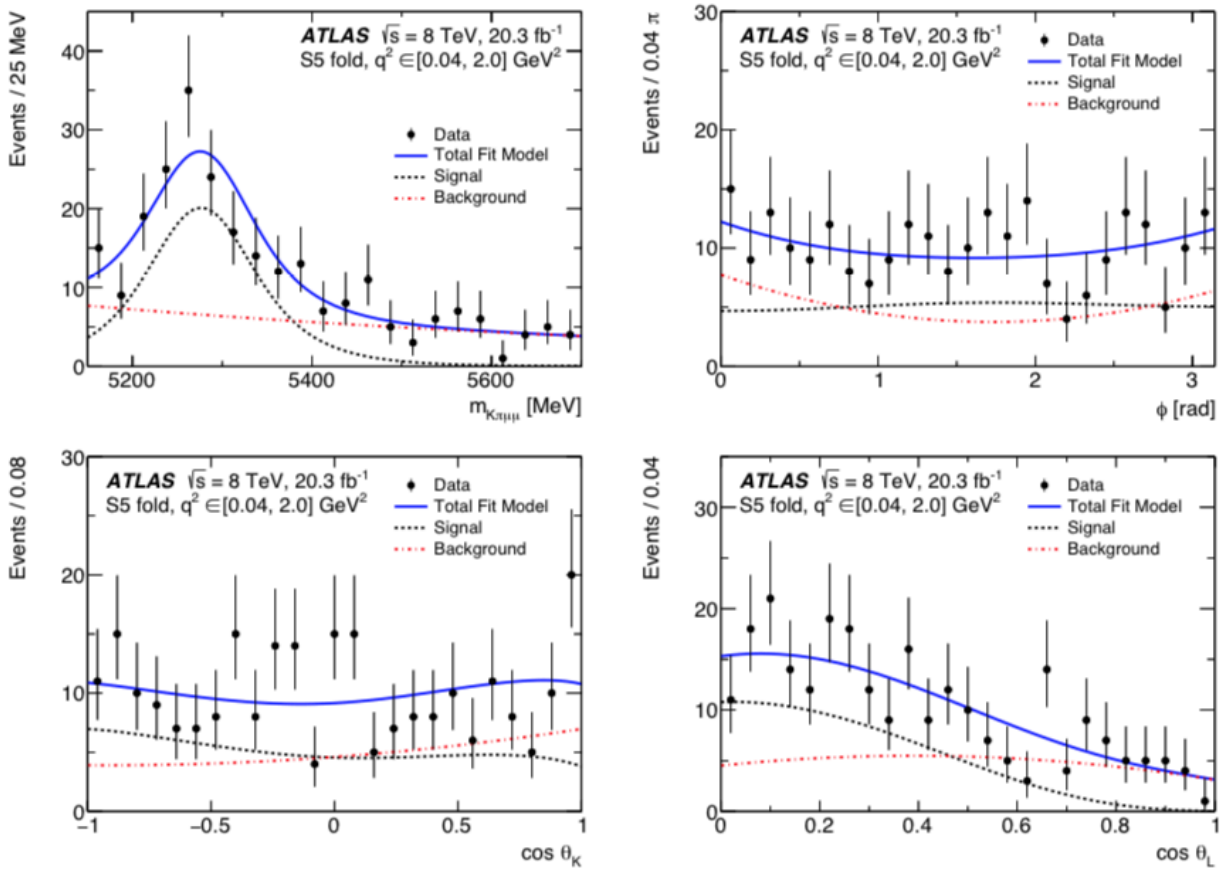

Statistically limited

JHEP 10 (2018) 047

$B^0 \rightarrow K^{*0}\mu^+\mu^-$ angular analysis

- CMS: fit signal, mistag signal and bkg
  - Fs, As, F_L fixed from previous measurements
  - P1, P5' fitted parameters
  - S-wave included in PDF
  - 1400 events in 7 q^2 bins
- Signal PDF folded to reduce the number of free parameters and improve fit convergence

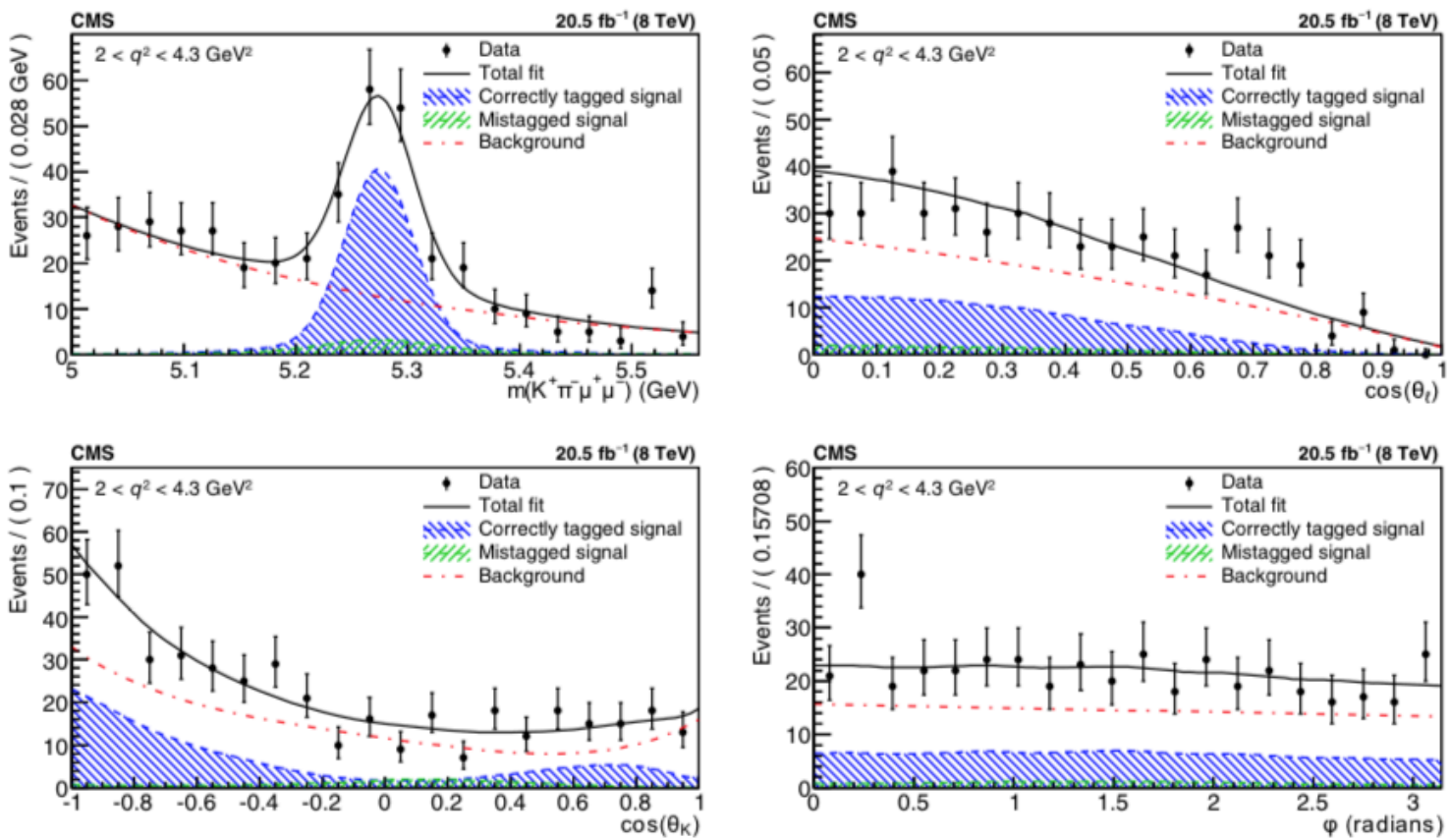

Statistically limited

Phys. Lett. B 781 (2018) 517

$B^0 \rightarrow K^{*0}\mu^+\mu^-$ angular analysis

- Theory:
  - DHMV/JC: QCD factorization, hadronic uncertainties from calculations
  - HEP t/CFFMPSV t: hadronic charm contributions fitted from LHCb data

- ATLAS generally in good agreement with SM, except a ~2.5σ deviation from DHMV for P_4', P_5' in one bin
  - LHCb sees a >3σ discrepancy on P'_5

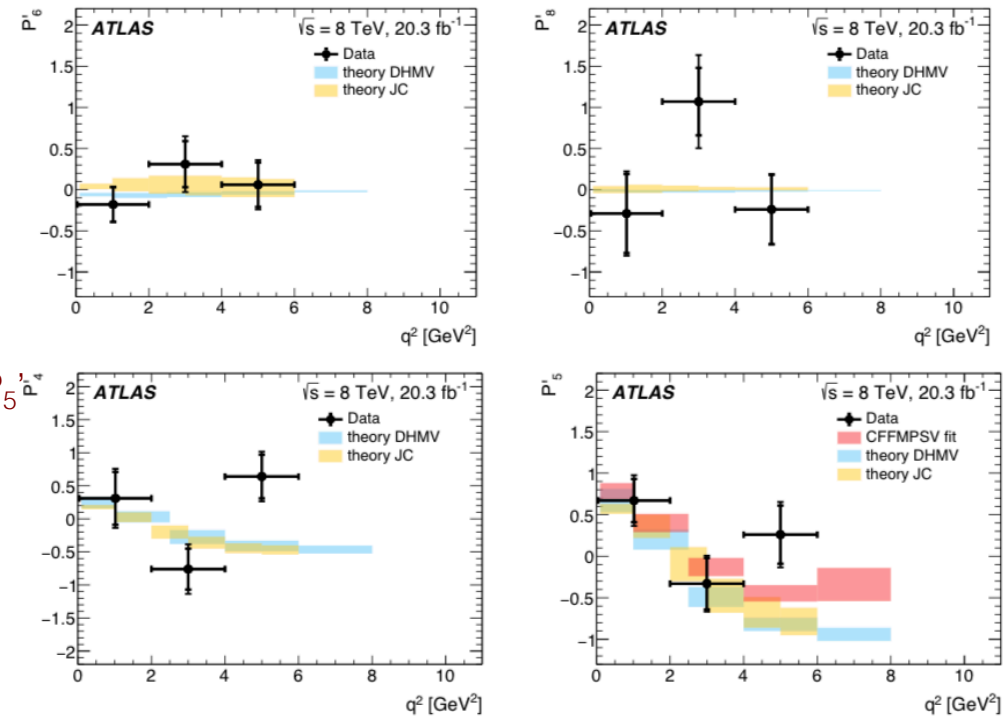

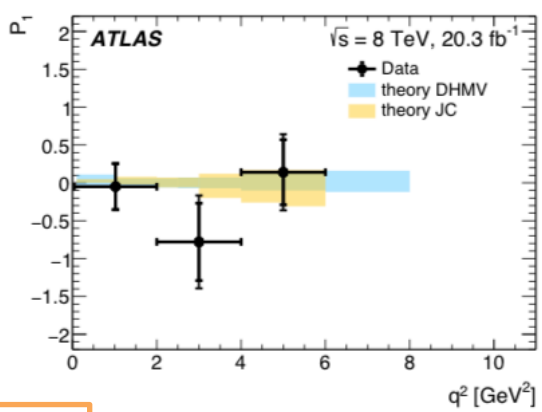

JHEP 10 (2018) 047

$B^0 \rightarrow K^{*0}\mu^+\mu^-$ angular analysis

- Theory:
  - DHMV/JC: QCD factorization, hadronic uncertainties from calculations
  - HEP t/CFFMPSV t: hadronic charm contributions fitted from LHCb data

- ATLAS generally in good agreement with SM, except a ~2.5σ deviation from DHMV for P_4', P_5' in one bin
  - LHCb sees a >3σ discrepancy on P'_5

- CMS data compatible with SM predictions in the whole range and favoring DHMV at low q^2

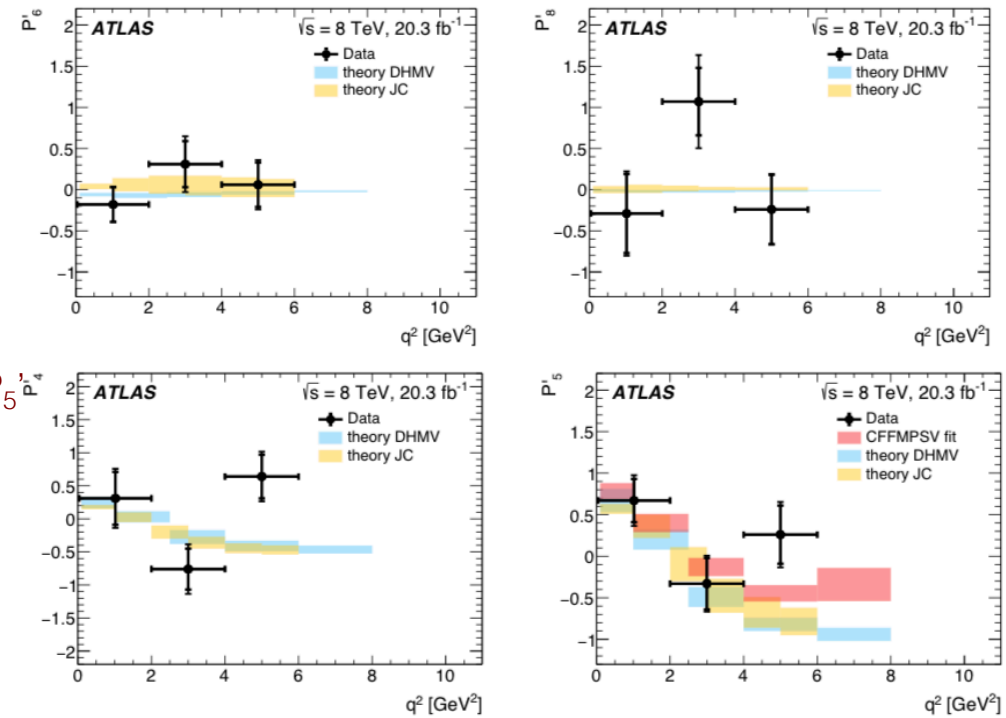

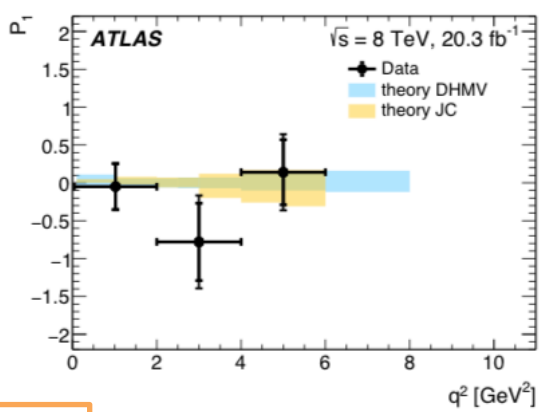

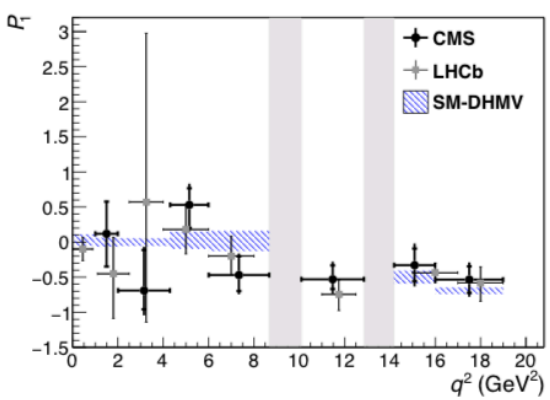

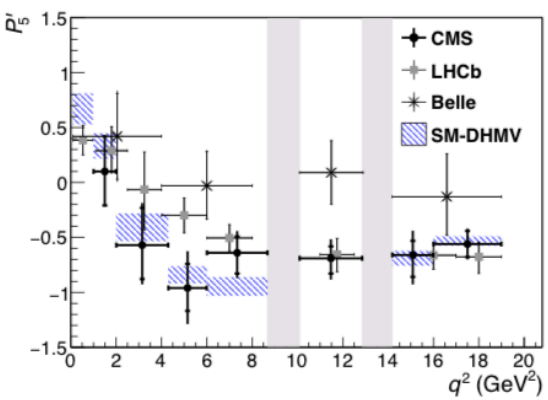

JHEP 10 (2018) 047

Phys. Lett. B 781 (2018) 517

$B^+ \rightarrow K^+\mu^+\mu^-$ angular analysis

- Decay rate depends on angle between the directions of μ^- and K^+ in the di-muon rest frame θ_L

$$\frac{1}{\Gamma_\ell}\frac{d\Gamma_\ell}{d\cos\theta_\ell} = \frac{3}{4}(1-F_H)(1-\cos^2\theta_\ell) + \frac{1}{2}F_H + A_{FB}\cos\theta_\ell$$

A_{FB} = Forward-backward Asymmetry
F_H = contribution from the pseudoscalar, scalar, and tensor amplitudes to the decay width

- Angular analysis in 7 q^2 bins ($1<q^2<22$ GeV^2)
- 2D unbinned max-likelihood fit: m(Kμμ) and $\cos\theta_l$
- N(B→Kμμ) = 2286±73

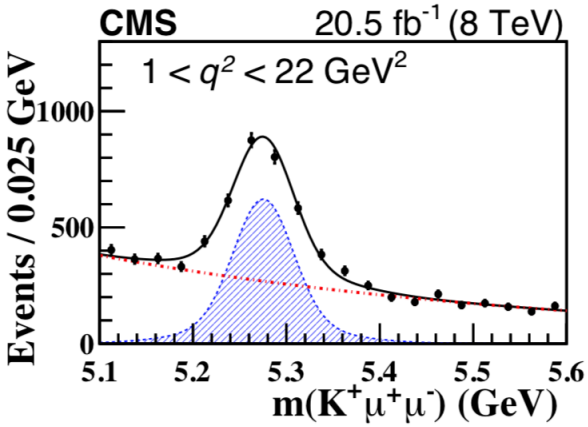

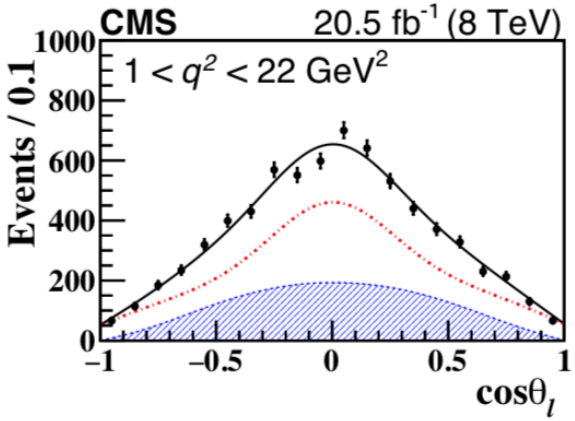

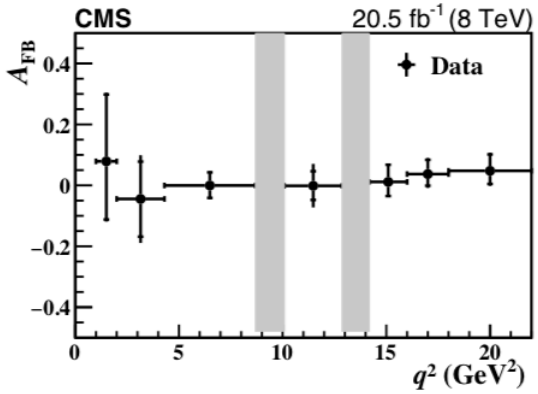

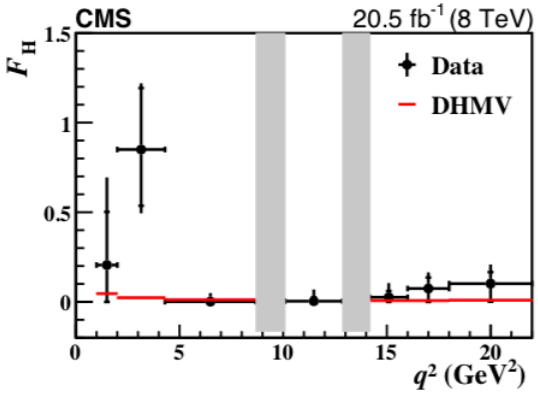

Results compatible with SM prediction and consistent with previous measurements

Phys. Rev. D 98 (2018) 112011

Search for $X^{\pm} \rightarrow B^0_s \pi^{\pm}$ resonance

- D0 published evidence of a (tetraquark) state X(5568) in the $B_s\pi^{\pm}$ spectrum via $B_s^0 \rightarrow J/\psi\ \phi$, $J/\psi \rightarrow \mu^+\mu^-$, $\phi \rightarrow K^+K^-$
- Also seen in semi-leptonic decays: $X^{\pm}(5568) \rightarrow B^0_s \pi^{\pm}$ where $B^0_s \rightarrow \mu^{\pm} D^{\pm}_s X$, $D^{\pm}_s \rightarrow \phi\pi^{\pm}$
- Not seen by LHCb, nor CDF
- ATLAS and CMS have enough statistic to observe a signal or set precise limits on production cross-section

Phys. Rev. Lett. 117, 022003 (2016)

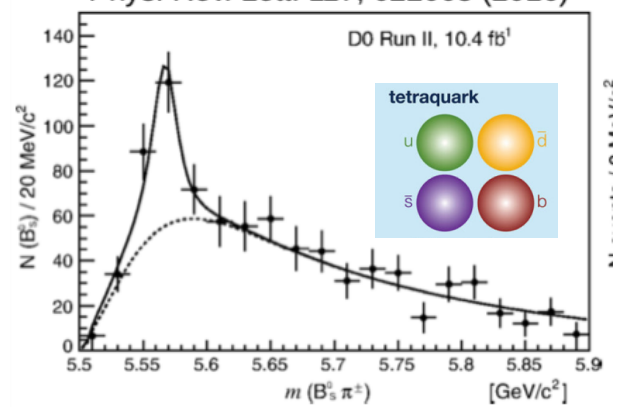

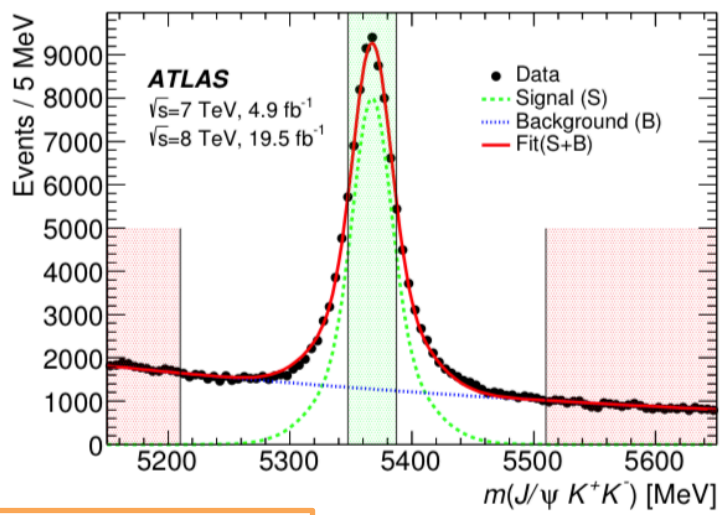

Phys. Rev. Lett. 120 (2018) 202007

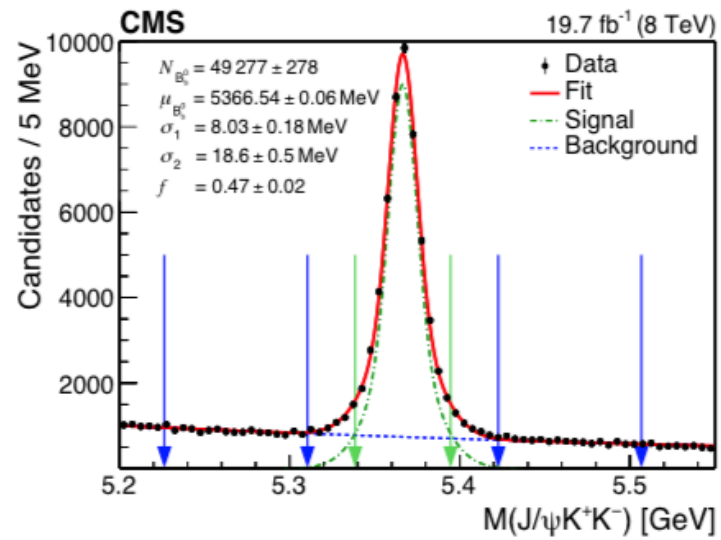

Phys. Rev. Lett. 120 (2018) 202005

ATLAS uses 4.9 fb^{-1} at 7 TeV + 19.5 fb^{-1} at 8 TeV data → $N(B^0_s) = 52750 \pm 280$

CMS uses 19.7 fb^{-1} at 8 TeV data → $N(B^0_s) = 49277 \pm 278$

Search for $X^{\pm} \rightarrow B^0_s \pi^{\pm}$ resonance

Phys. Rev. Lett. 120 (2018) 202007

Phys. Rev. Lett. 120 (2018) 202005

- $B^0_s \pi^{\pm}$ candidates selected by requiring a charged track, with p_T>500 MeV + track quality cuts, from the same PV as the B^0_s
- Analysis repeated for $p_T(B^0_s)$>10 GeV and for $p_T(B^0_s)$>15 GeV
- Invariant mass of the $B^0_s \pi^{\pm}$ candidates (re)defined as (improving mass resolution):

$$M^{\Delta}(B^0_s \pi^{\pm}) = M(J/\psi K^+ K^- \pi^{\pm}) - M(J/\psi K^+ K^-) + m_{B^0_s}$$

Number of $X^{\pm}$ candidates from unbinned max-likelihood fit

	N(X) $p_T(B^0_s)$>10 GeV	N(X) $p_T(B^0_s)$>15 GeV
ATLAS	60±140	30±150
CMS	-85±160	-103±122

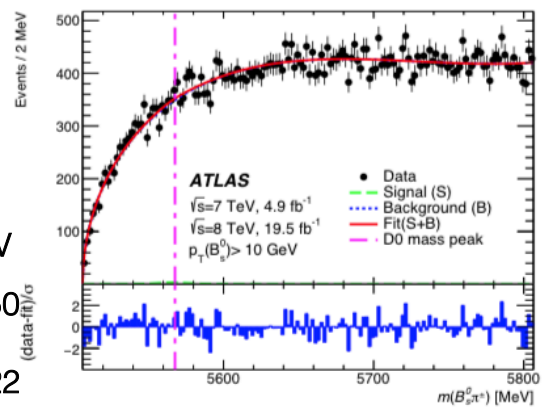

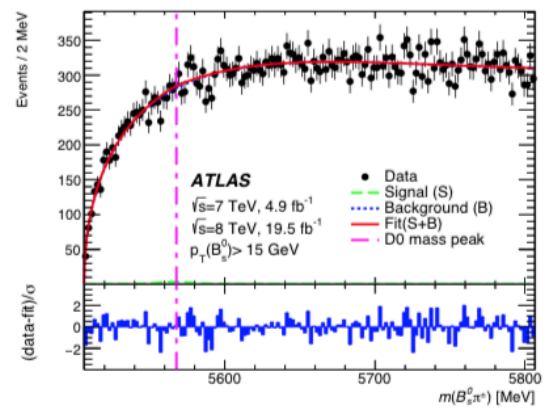

No signal evidence

Both experiments can set upper limits

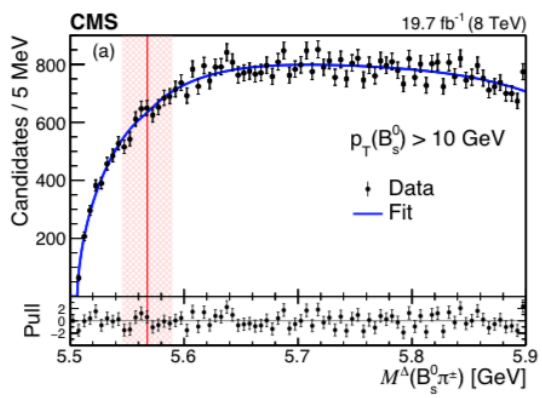

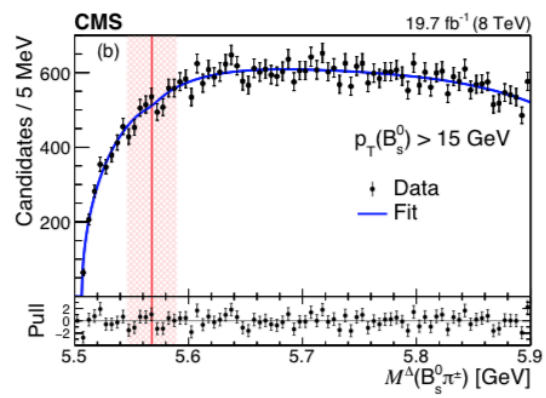

Search for $X^{\pm} \rightarrow B^0_s \pi^{\pm}$ resonance

- Upper limits set to ρX, the cross-section ratio of X(5568) to B^0_s

$$\rho_X \equiv \frac{\sigma(pp \to X + \text{anything})\, \mathcal{B}(X \to B^0_s \pi^{\pm})}{\sigma(pp \to B^0_s + \text{anything})} = \frac{N_X}{\epsilon_{rel} N_{B^0_s}}$$

- Asymptotic CLs method

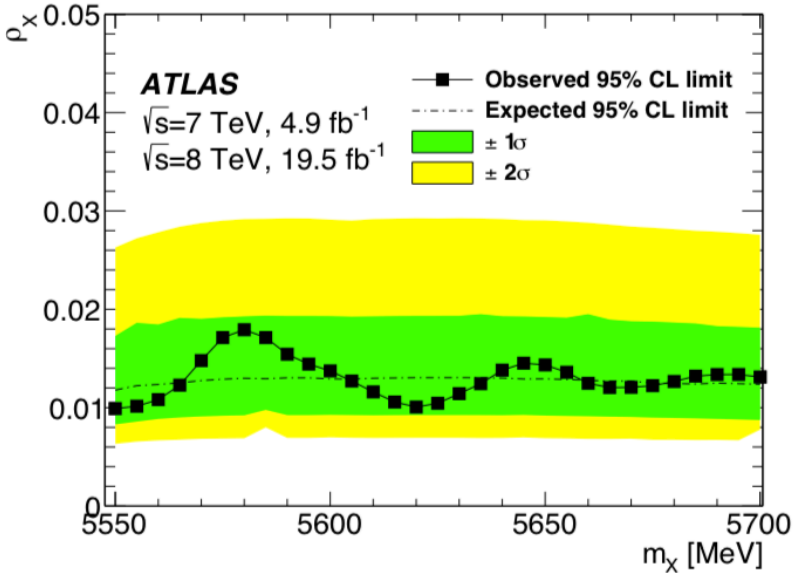

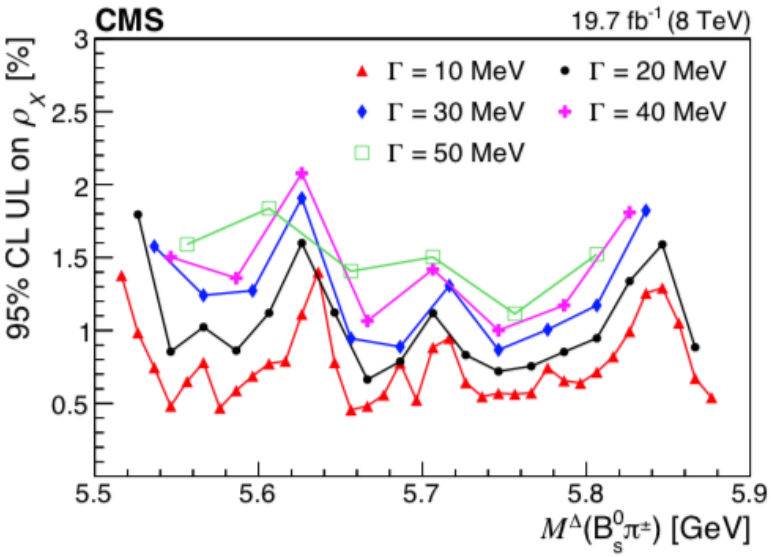

$\rho_X < 1.5\%$ at 95% CL for $p_T(B^0_s) > 10$ GeV
$\rho_X < 1.6\%$ at 95% CL for $p_T(B^0_s) > 15$ GeV

$\rho_X < 1.1\%$ at 95% CL for $p_T(B^0_s) > 10$ GeV
$\rho_X < 1.0\%$ at 95% CL for $p_T(B^0_s) > 15$ GeV

Phys. Rev. Lett. 120 (2018) 202007

Phys. Rev. Lett. 120 (2018) 202005

B_c^+ ground and excited states

- Weakly decaying particle consisting of two heavy quarks
- Spectrum and properties of B_c^+ family are predicted by non-relativistic potential models, perturbative QCD and lattice calculations
- Measurements of the ground and excited states → test of these predictions

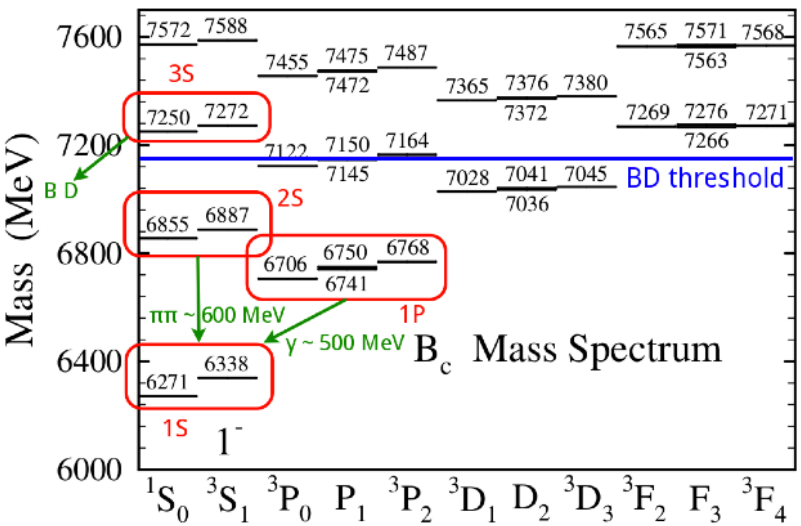

- In 2016 ATLAS published the first observation of state $B_c^+(2S)$ state at a mass:

  $M = 6842 \pm 4(stat) \pm 5(syst)$ MeV
  - Consistent with the prediction
  - 5.2σ including 7 and 8 TeV data
  - Not resolving the two B_c^+ (2S)and B_c^{*+}(2S) states
- New evidence from LHCb
- New results from CMS
  - Observation of two excited B_c^+ states
  - Measurement of B_c^+ (2S) mass

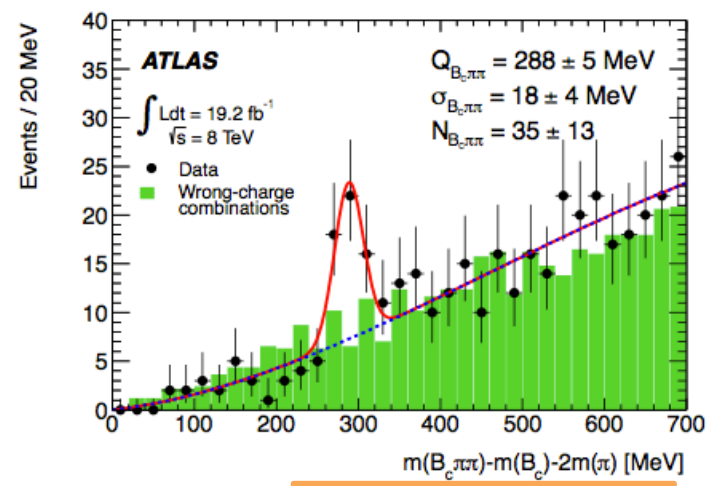

Phys. Rev. Lett. 113 (2014) 212004

B_c^+ excited states

Phys. Rev. Lett. 122 (2019) 132001

- Observation of signals consistent with $B_c^+(2S)$ and $B_c^{*+}(2S)$ in the decay channel
  $B_c^+(2S) \rightarrow B_c^+\pi^+\pi^- \rightarrow J/\psi\ \pi^+\pi^+\pi^-$
  $B_c^{(*)+}(2S) \rightarrow B^*_c{}^+\pi^+\pi^- \rightarrow B_c^+(\gamma)\ \pi^+\pi^- \rightarrow J/\psi\ \pi^+(\gamma)\ \pi^+\pi^-$
  - B_c^+ reconstruction: di-muon constrained to J/ψ mass + high purity charged track as π
  - $B_c^+(2S)$ and $B_c^{*+}(2S)$ reconstruction: kinematic fit of B_c^+ with 2 oppositely charged particles from the same vertex
- Low energetic γ from $B^*_c \rightarrow B_c^+\gamma$ difficult to detect
  → $B_c^{*+}(2S)$ peak in the $B_c^+\pi^+\pi^-$ mass spectrum seen at a mass lower than $M(B_c^+(2S))$ → double peak structure

143 fb^{-1} at 13 TeV data

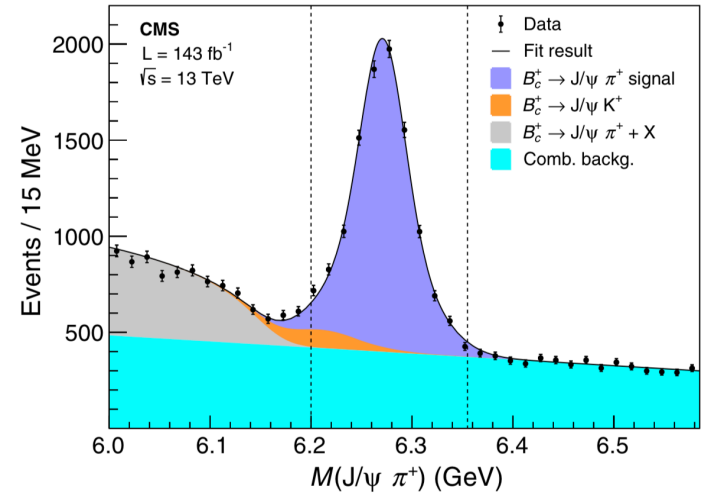

- Good separation of the two states
- $N(B_c^+(2S))=67\pm10$;
  $N(B_c^{*+}(2S))=51\pm10$;
  $\Delta M=29.1\pm1.5$ MeV

First measurement of
$M(B_c^+(2S)) = 6871.0\pm1.2(stat)\pm0.8(syst)\pm0.8(B_c^+)$ MeV

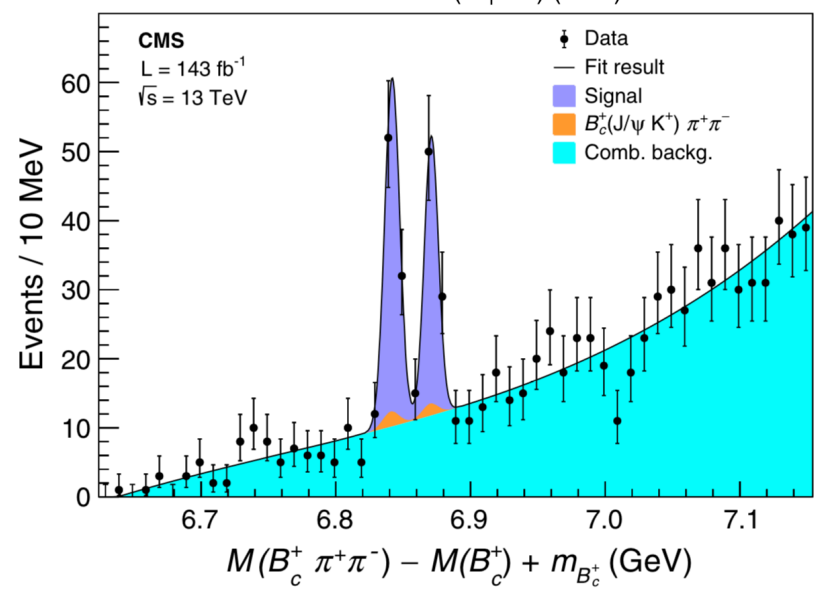

Observation of Z→J/ψ l^+l^- decay

- Valuable measurement for calculation of the fragmentation function for a virtual photon to split into a J/ψ
- Background for H→quarkonia decays accessible in future
- Analysis in e and μ channels (ll = ee or μμ)

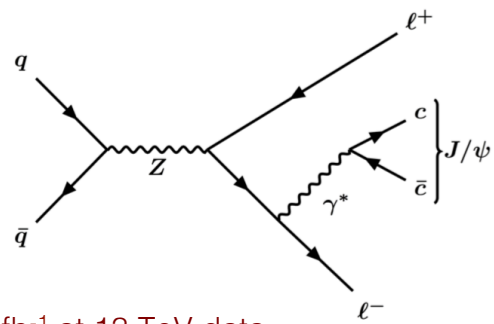

CMS: 35.9 fb^{-1} at 13 TeV data

Fiducial region

$$40 < m_{\ell^+\ell^-} < 80\,\text{GeV}$$
$$|\eta(\text{electrons})| < 2.5, \quad |\eta(\text{muons})| < 2.4$$
$$p_T(\ell_1, \ell_2, \mu, \mu) > (30, 15, 3.5, 3.5)\,\text{GeV}$$
$$\text{Signal: } p_T^{J/\psi} > 8.5\,\text{GeV}$$
$$\text{Reference channel: } 4 < m(\mu^\pm\mu^\mp) < 80\,\text{GeV}$$

Ratio of exclusive Z→J/ψ l^+l^- decay to inclusive Z→4μ (partial cancellation of systematics)

$$\mathcal{R}_{J/\psi\ell^+\ell^-} = \frac{\mathcal{B}(Z \to J/\psi\,\ell^+\ell^-)}{\mathcal{B}(Z \to \mu^+\mu^-\mu^+\mu^-)}$$

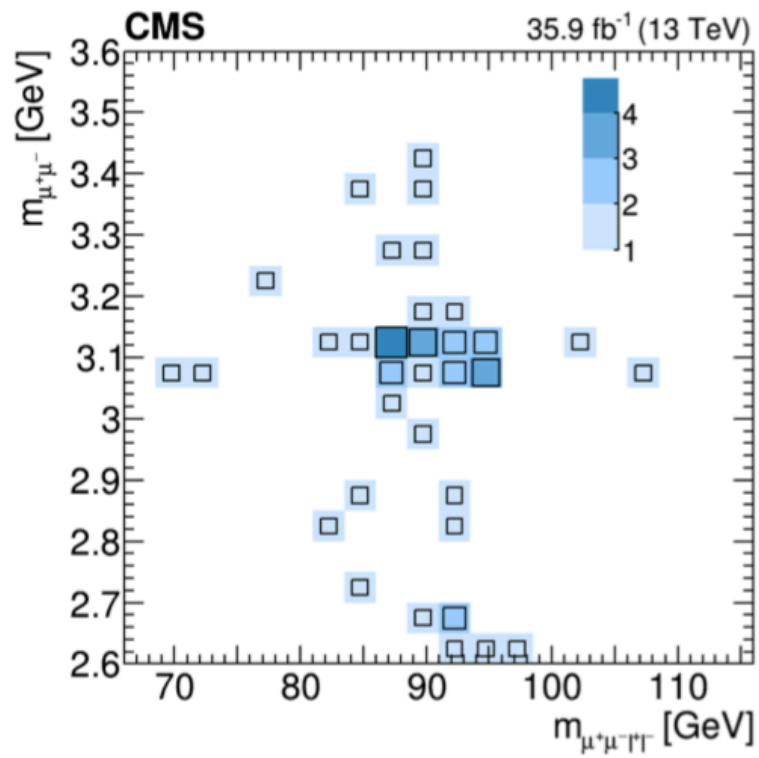

Phys. Rev. Lett. 121 (2018) 141801

Observation of Z→J/ψ l^+l^- decay

Yields from fits:

N(Z→ψμμ) = 13.0±3.9

N(Z→ψee) = 11.2±3.4

$$\mathcal{R}_{J/\psi\,\ell^+\ell^-} = 0.67 \pm 0.18\,(\text{stat}) \pm 0.05\,(\text{syst})$$

Assumption of unpolarised J/ψ (full polarisation change the result by <25%)

$$\mathfrak{B}(Z \to J/\psi\, l^+l^-) \approx 8 \times 10^{-7}$$

Consistent with predictions ($6.7\pm0.7\times10^{-7}$ and 7.7×10^{-7})

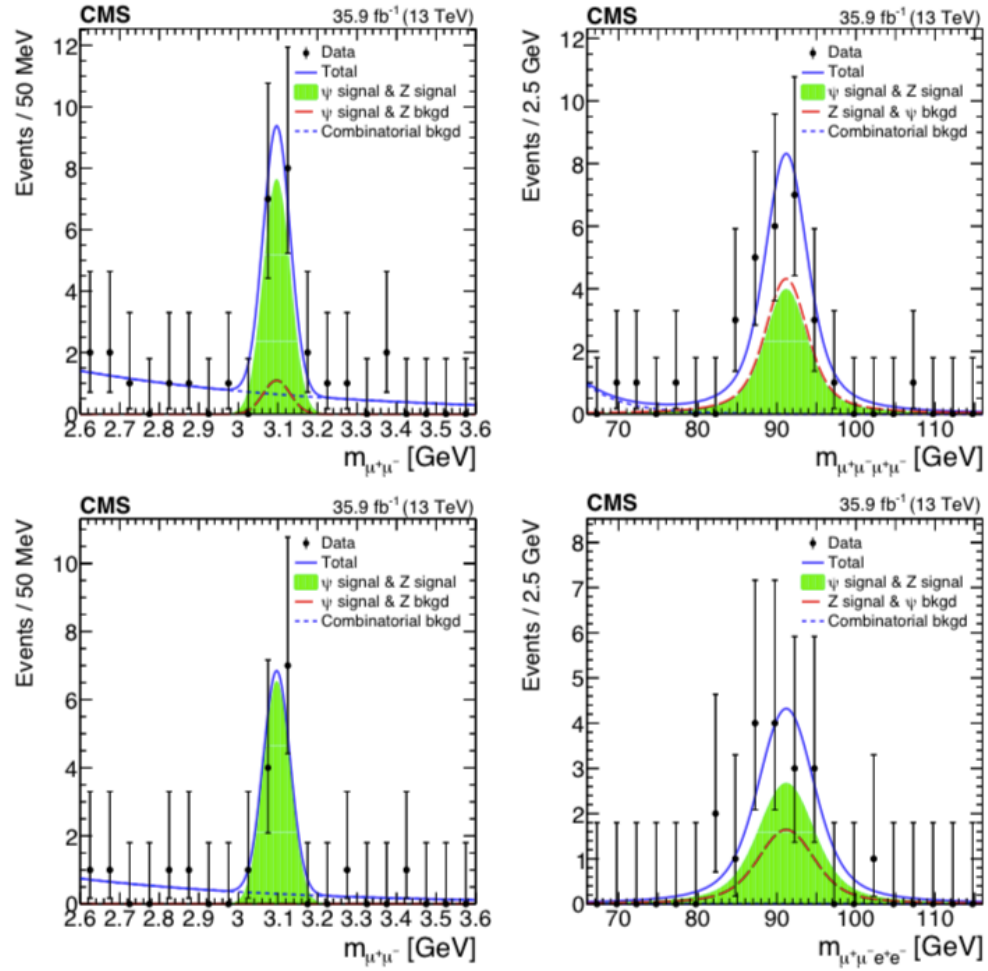

Phys. Rev. Lett. 121 (2018) 141801

Summary

- ATLAS and CMS have a rich physics program for studies of heavy flavor physics

- Selection of recent results on:
- Quarkonia production
  - Good general agreement with predictions
  - Measurement of Nuclear Modification Factors in pPb and PbPb collisions → CNM effects relevant for Y in low p_T region
  - σ_{eff} generally lower from prompt di-J/ψ and di-Y wrt other final states
- $B^0 \rightarrow K^+\pi^-\mu^+\mu^-$ angular analysis:
  - CMS compatible with expectations; ATLAS has tension of ~2.5σ in 1 q^2 bins for P'_4 and P'_5
- $B^+ \rightarrow K^+\mu^+\mu^-$ angular analysis
  - Compatible with SM predictions
- Search for $X^\pm(5568) \rightarrow B^0_s\pi^\pm$ resonance
  - No evidence; strong limits set on cross-section
- B_c^+ ground and excited states
  - First measurement of $M(B_c^+(2S)) = 6871.0 \pm 1.2(stat) \pm 0.8(syst) \pm 0.8(B_c^+)$ MeV
- Observation of $Z \rightarrow J/\psi\, l^+l^-$ decay

Many more studies ongoing; more results to come in the next months

Additional Material

Data set

- LHC runs
  - Run1 (2009-2012)
  - Run2 (2015-2018)
- Excellent data taking performance
  - ~160 fb^{-1} data at pp collisions collected by each experiments at 13 TeV
  - 7 and 8 TeV data in Run1
  - pPb and PbPb runs

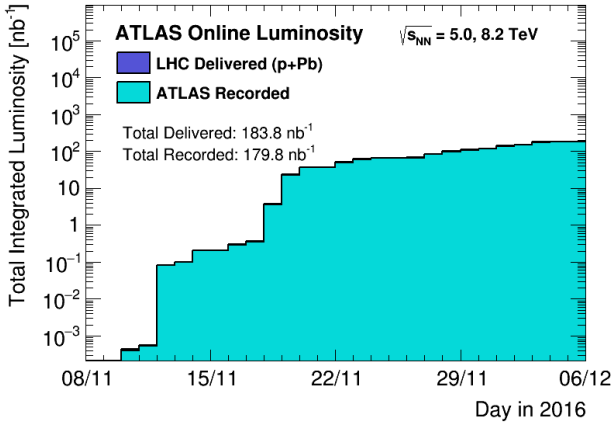

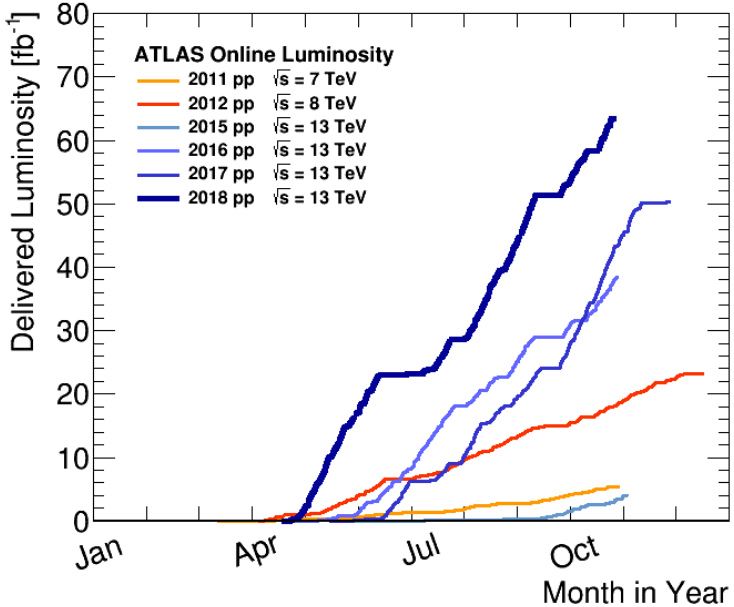

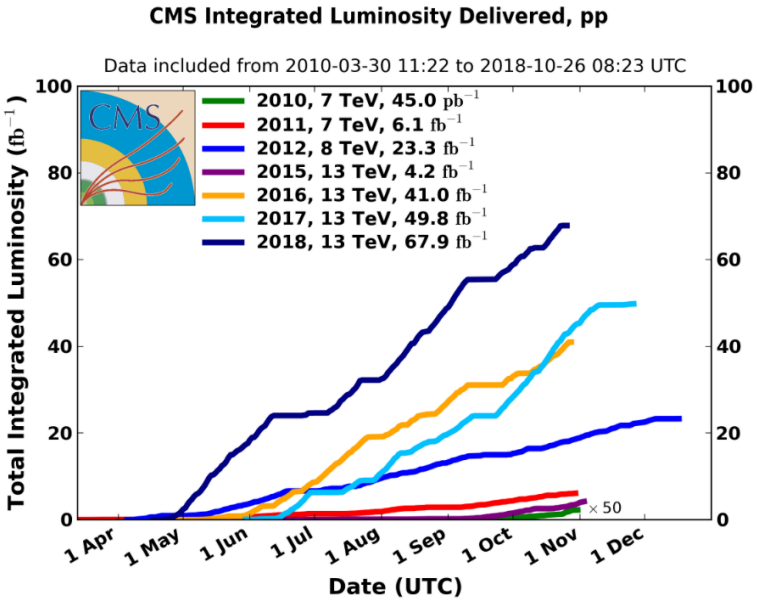

General purpose experiment with very good potential for Heavy Flavor physics

Non-prompt J/ψ and ψ(2S) in pp

Non-prompt J/ψ at 5.02 TeV

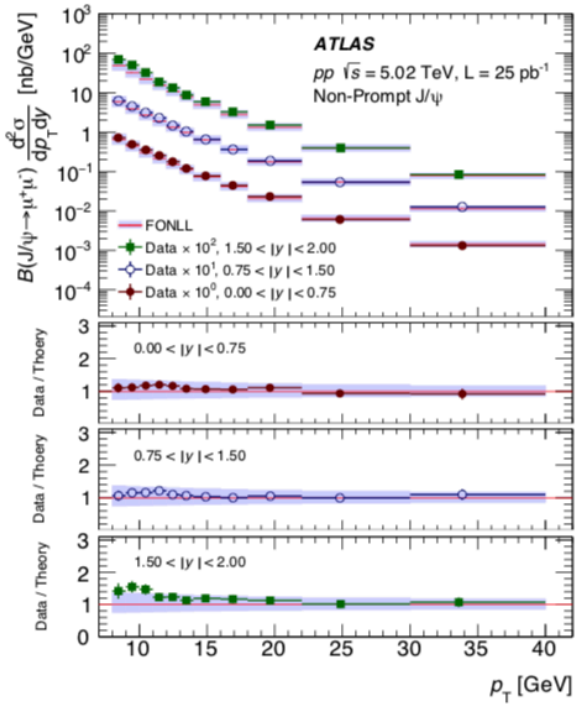

Non-prompt ψ(2S) at 5.02 TeV

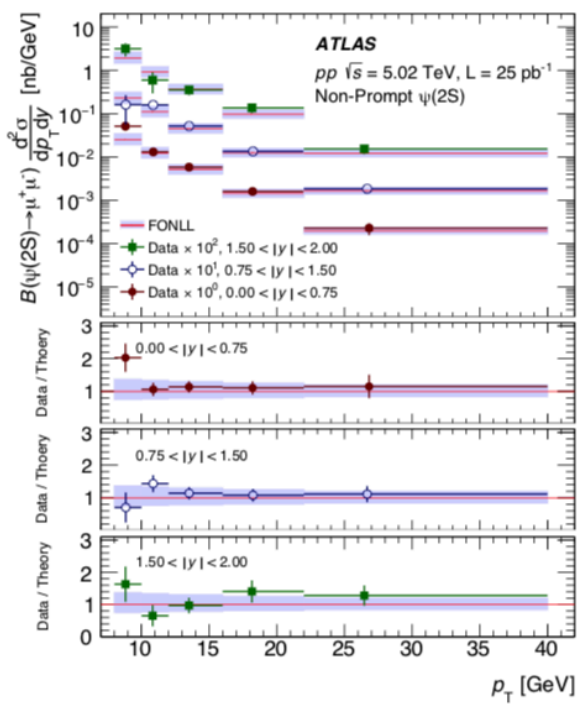

- Good description of the data by FONLL (non-prompt) calculations in the full p_T range

Non-prompt J/psi 7 and 8 TeV - ATLAS

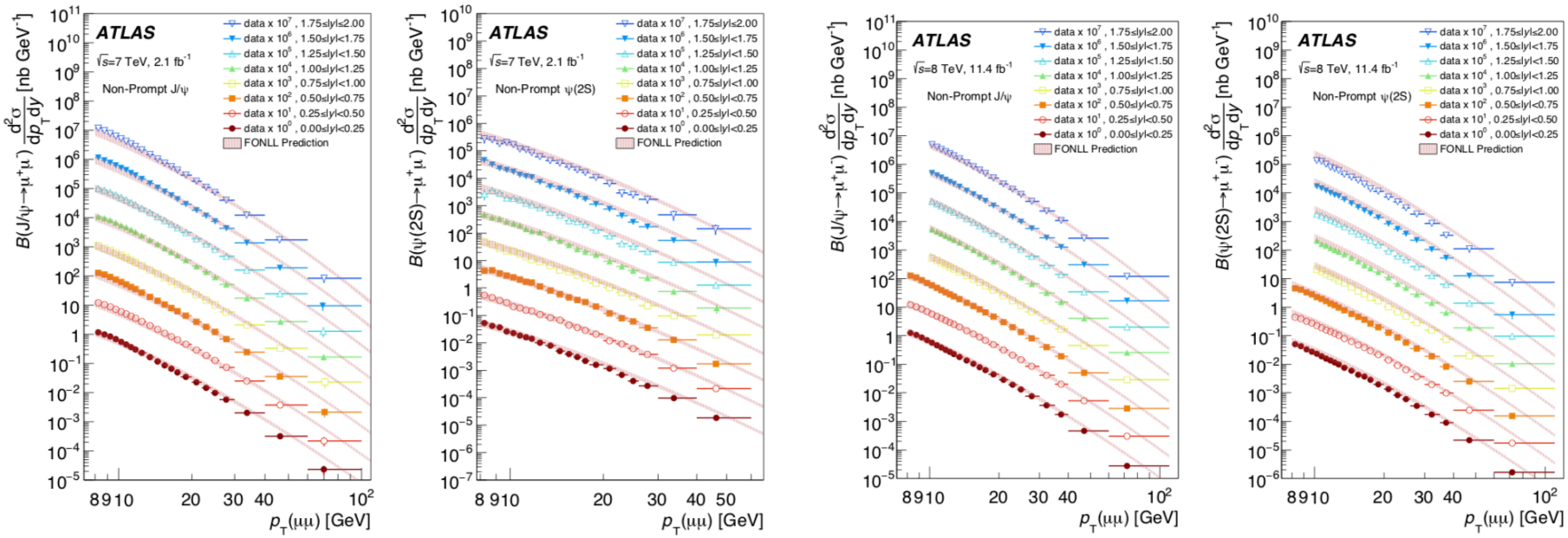

- Good description of the data by FONLL calculations in the full pT range

J/ψ, ψ(2S), Υ production systematics

- ATLAS

Collision type	Sources	Ground-state yield [%]	Excited-state yield [%]	Ratio [%]
p+Pb collisions	Luminosity	2.7	2.7	–
	Acceptance	1–4	1–4	–
	Muon reco.	1–2	1–2	< 1
	Muon trigger	4–5	4–5	< 1
	Charmonium fit	2–5	4–10	7–15
	Bottomonium fit	2–15	2–15	5–12
pp collisions	Luminosity	5.4	5.4	–
	Acceptance	1–4	1–4	–
	Muon reco.	1–5	1–5	< 1
	Muon trigger	5–7	5–7	< 1
	Charmonium fit	2–7	4–10	7–11
	Bottomonium fit	1–15	2–15	5–12

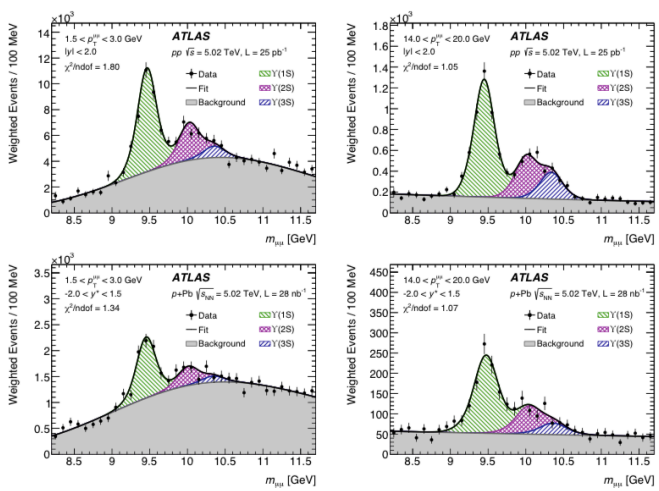

- CMS

Lumi	2.3%
Acceptance	3.0%
Muon eff (J/ψ, ψ(2S)	2.5%
Muon eff (Υ(nS))	1.8%
Muon trigger	3%
Fit model	2.0%

Nuclear Modification Factors

Eur. Phys. J. C 78 (2018) 171

- Comparison with ALICE (J/psi) and ALICE and LHCb (Υ): pPb collisions

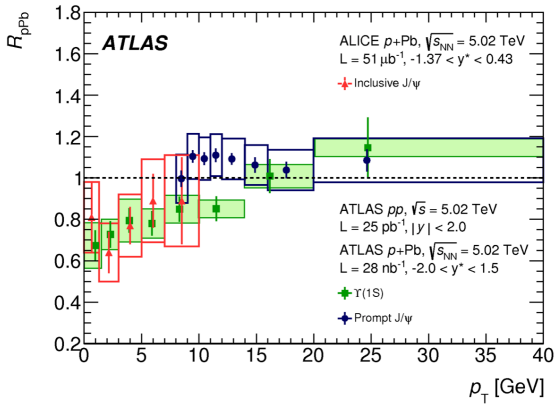

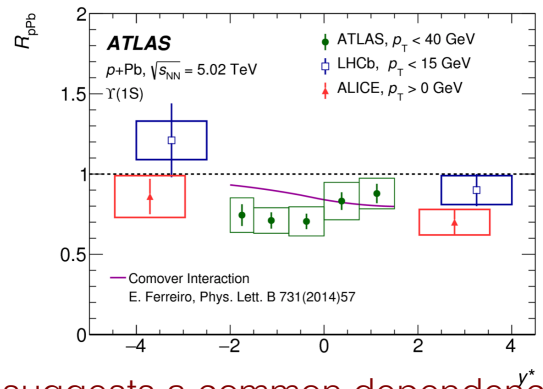

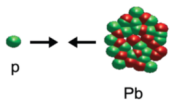

suggests a common dependence on y*

- Comparison between R_{pPb} and R_{PbPb} for prompt and non-prompt J/ψ
  - Very strong suppression of charmonia production in PbPb collisions
  - Similar for prompt and non-prompt J/ψ production

Eur. Phys. J. C 78 (2018) 762

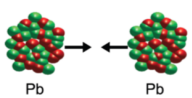

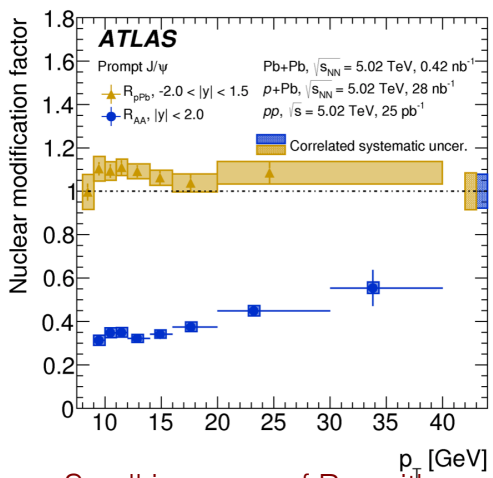

Small increase of R_{AA} with p_T in prompt J/ψ production

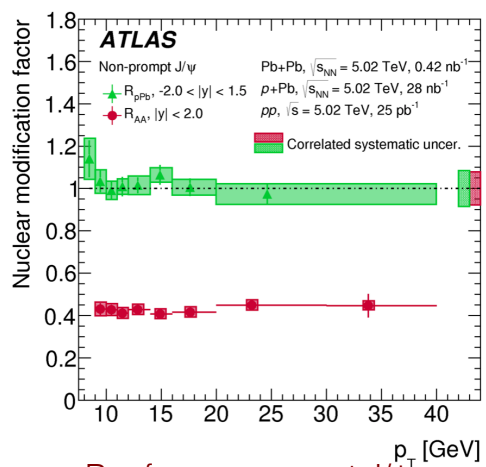

R_{AA} for non-prompt J/ψ production ~constant

- R_{AA} vs N_{jets} in PbPb collisions

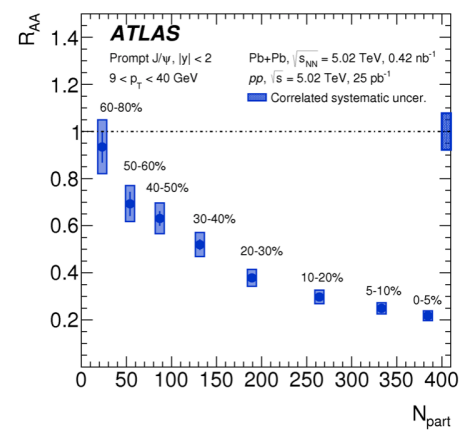

Suppression decreases going from central to peripheral collisions

Di-J/ψ production at 8 TeV

Eur. Phys. J. C 77 (2017) 76

ATLAS: 11.4 fb^{-1} at 8 TeV pp

- Two prompt J/ψ → μμ decays from the same pp collision
  - Invariant mass fit
  - Pseudo-proper decay time fits → prompt-prompt
  - Vertex d_Z fit → two J/ψ from the same vertex (pileup-removal)
- Data driven SPS contribution
- Analysis in two regions according to sub-leading J/ψ_2 rapidity

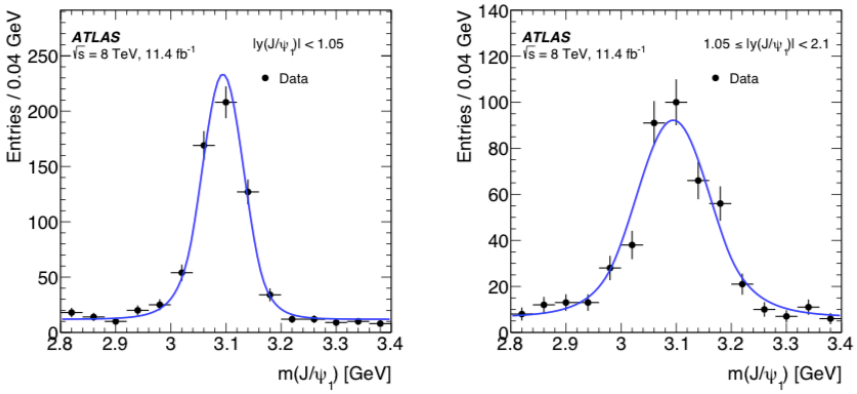

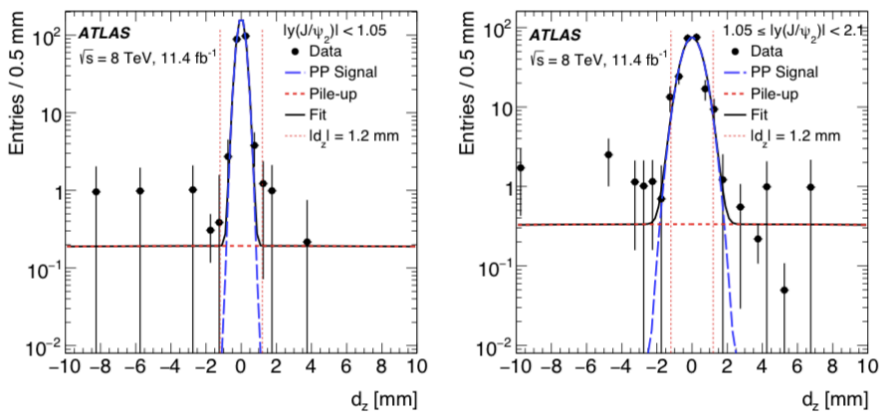

$$|y^*_{J/\psi_2}| < 1.05 \qquad 1.05 < |y^*_{J/\psi_2}| < 2.1$$

$$N_{J/\psi J/\psi} = 3310 \pm 330 \qquad N_{J/\psi J/\psi} = 3140 \pm 370$$

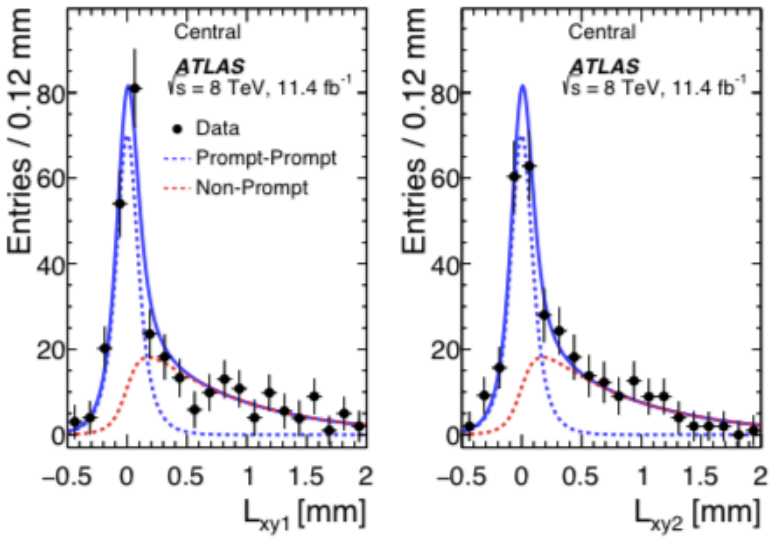

Di-J/ψ production at 8 TeV

Eur. Phys. J. C 77 (2017) 76

- DPS vs SPS undistinguishable on event-by-event base
- Different overall kinematics → angular correlation (Δy and Δφ)
- Events re-weighted according to Δy-Δϕ bin

SPS

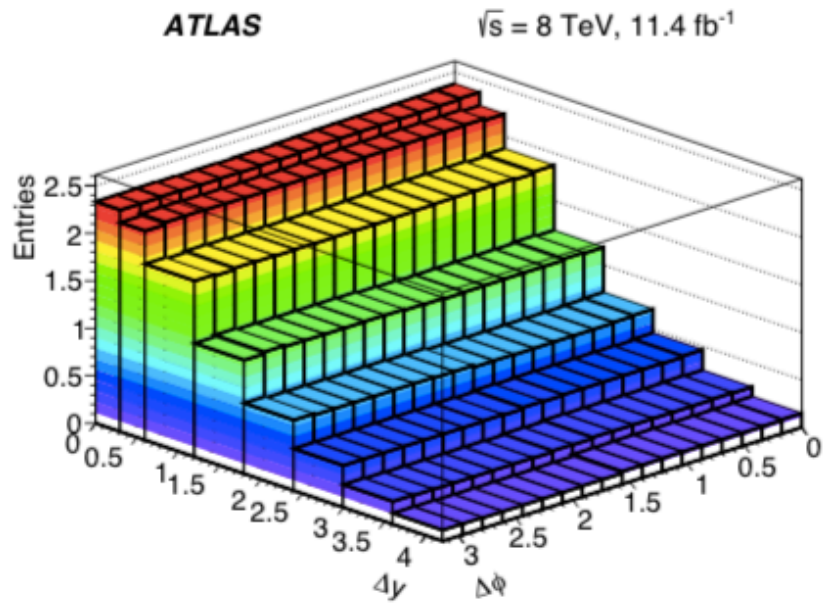

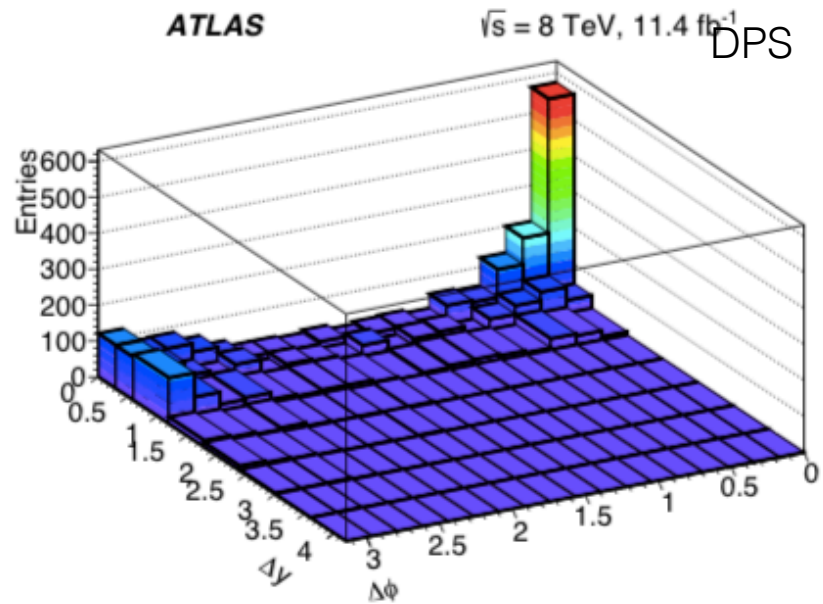

Di-J/ψ production at 8 TeV

Eur. Phys. J. C 77 (2017) 76

- Theory plots for inclusive acceptance, not for fiducial one (scale factor ~6)

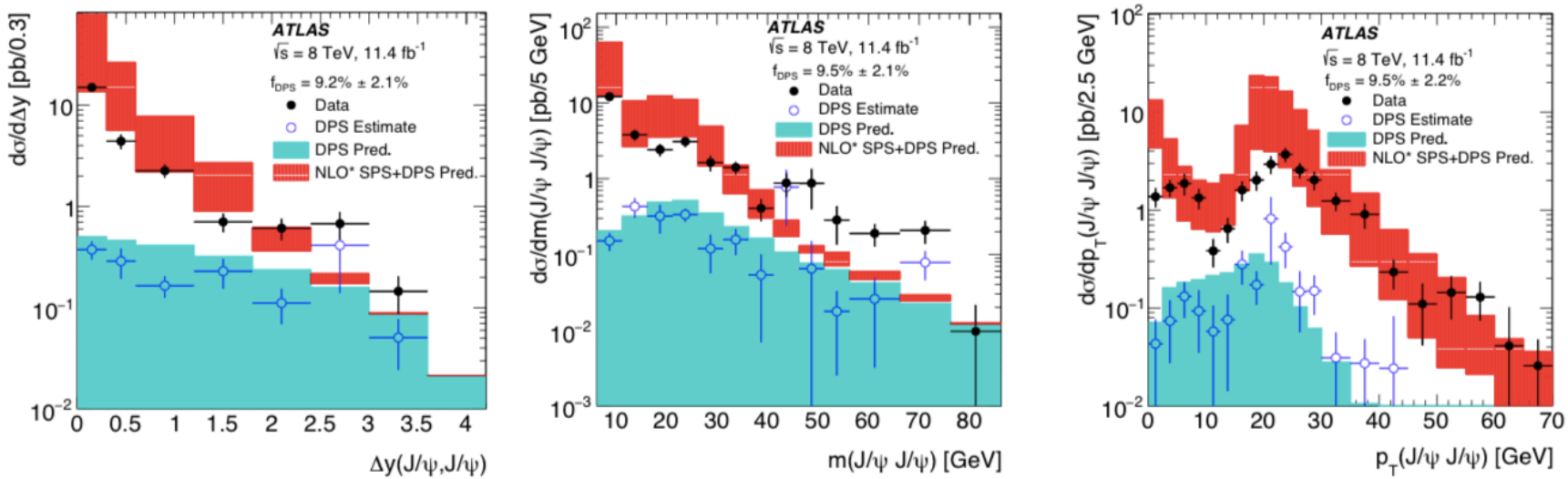

Di-J/ψ production at 8 TeV

- Systematics

Systematic uncertainty: di-J/ψ cross-section [%]		
Source	$\lvert y(J/\psi_2)\rvert < 1.05$	$1.05 \leq \lvert y(J/\psi_2)\rvert < 2.1$
Trigger	±7.5	±8.3
Muon reconstruction	±1.1	±1.3
Kinematic acceptance	±0.4	±1.1
Mass model	±0.1	±0.1
Mass bias	±0.2	±0.2
Prompt–prompt model	±0.2	±0.01
Differential f_{PP} corr.	±0.6	±0.3
Pile-up	±0.03	±0.4
Total	± 7.7	± 8.5
Branching fraction	±1.1	
Luminosity	±1.9	

Systematic uncertainty: f_{DPS} [%]	
Source	Relative uncertainty [%]
Trigger	±0.7
Muon reconstruction	±0.1
Mass model	±0.01
Mass bias	±0.02
Prompt–prompt model	±0.1
Differential f_{PP} corr.	±0.1
Pile-up	±0.8
DPS model	±5.6
Total	± 5.7

Di-J/ψ production at 8 TeV

- Spin-alignment

Maximum spin-alignment scenarios: di-J/ψ cross-section		
Scenario	$\lvert y(J/\psi_2)\rvert \leq 1.05$	$1.05 \leq \lvert y(J/\psi_2)\rvert < 2.1$
Longitudinal	-47%	-45%
Transverse positive	+68%	+82%
Transverse negative	+39%	+28%
Transverse zero	+51%	+47%

Maximum spin-alignment scenarios: di-J/ψ DPS cross-section		
Scenario	$\lvert y(J/\psi_2)\rvert \leq 1.05$	$1.05 \leq \lvert y(J/\psi_2)\rvert < 2.1$
Longitudinal	-47%	-45%
Transverse positive	+79%	+65%
Transverse negative	+35%	+35%
Transverse zero	+54%	+48%

Υ(1S) pair production at 8 TeV

JHEP 05 (2017) 013

- Systematics

Component	Uncertainty (%)
Resonance shape	7.9
Simulation	4.9
Efficiency	3.7
Acceptance	2.8
Integrated luminosity	2.6
Total	10.7

Effects of polarisation

$\lambda_{\theta 1}$	+1	+1	+0.5	−0.5	+0.5	−1	+1	−0.5	−0.5	−1
$\lambda_{\theta 2}$	+1	+0.5	+0.5	+0.5	−0.5	+1	−1	−0.5	−1	−1
Change (%)	+36	+26	+18	−2	−3	−9	−9	−19	−29	−38

$B^0 \rightarrow K^{*0}\mu^+\mu^-$ angular analysis

- $B^0 \rightarrow K^{*0}\mu^+\mu^- \rightarrow K^+\pi^-\mu^+\mu^-$ is a FCNC process
- The process can be fully described by the three angles (θ_L, θ_K, ϕ) and the dimuon invariant mass squared q^2
- New physics entering the loop can be detected by looking at the **angular** distributions of the decay
- Angular differential decay rate expressed with S coefficients that may be represented by helicity or transversity amplitudes:

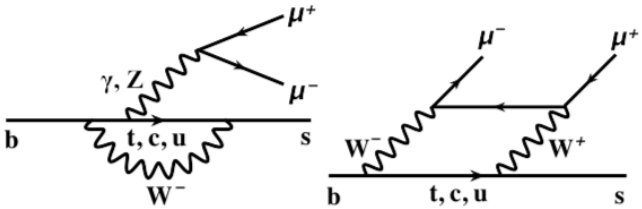

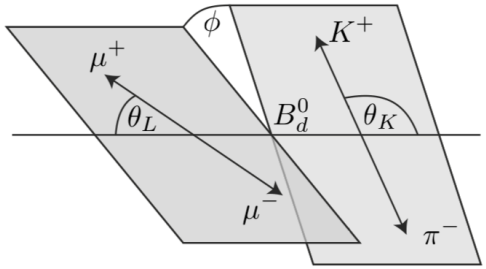

$$\frac{1}{d\Gamma/dq^2}\frac{d^4\Gamma}{d\cos\theta_L d\cos\theta_K d\phi dq^2} = \frac{9}{32\pi}\Bigg[\frac{3(1-F_L)}{4}\sin^2\theta_K + F_L\cos^2\theta_K + \frac{1-F_L}{4}\sin^2\theta_K\cos 2\theta_L$$
$$-F_L\cos^2\theta_K\cos 2\theta_L + S_3\sin^2\theta_K\sin^2\theta_L\cos 2\phi$$
$$+S_4\sin 2\theta_K\sin 2\theta_L\cos\phi + S_5\sin 2\theta_K\sin\theta_L\cos\phi$$
$$+S_6\sin^2\theta_K\cos\theta_L + S_7\sin 2\theta_K\sin\theta_L\sin\phi$$
$$+S_8\sin 2\theta_K\sin 2\theta_L\sin\phi + S_9\sin^2\theta_K\sin^2\theta_L\sin 2\phi\Bigg]. \quad (1)$$

$$P_1 = \frac{2S_3}{1-F_L}$$
$$P_2 = \frac{2}{3}\frac{A_{FB}}{1-F_L}$$
$$P_3 = -\frac{S_9}{1-F_L}$$
$$P'_{j=4,5,6,8} = \frac{S_{i=4,5,7,8}}{\sqrt{F_L(1-F_L)}}.$$

$A_{FB} = 3S_6/4$ Forward-backward Asymmetry
F_L = fraction of longitudinally polarised K*
F_S = s-wave fraction

- Generally written in terms of P and P' observables as they are less sensitive to theoretical uncertainties at LO
- LHCb measured a >3σ discrepancy with model on P'_5

ATLAS and CMS analysis uses ~20 fb^{-1} of 8 TeV pp data taken in 2012
ATLAS extracts P_1 and P'_i (i=4,5,6,8); CMS extracts P_1 and P'_5

$B^0 \rightarrow K^{*0}\mu^+\mu^-$ angular analysis

- Systematics

Systematic uncertainty	$F_L(10^{-3})$	$A_{FB}(10^{-3})$	$d\mathcal{B}/dq^2$ (%)
Simulation mismodeling	1–17	0–37	1.0–5.5
Fit bias	0–34	2–42	—
MC statistical uncertainty	3–10	5–18	0.5–2.0
Efficiency	34	5	—
$K\pi$ mistagging	1–4	0–7	0.1–4.1
Background distribution	20–36	12–31	0.0–1.2
Mass distribution	3	1	3.2
Feed-through background	0–27	0–5	0.0–4.0
Angular resolution	6–24	0–5	0.2–2.1
Normalization to $B^0 \rightarrow J/\psi K^{*0}$	—	—	4.6
Total systematic uncertainty	41–65	18–74	6.4–8.6

- Diff. cross-section

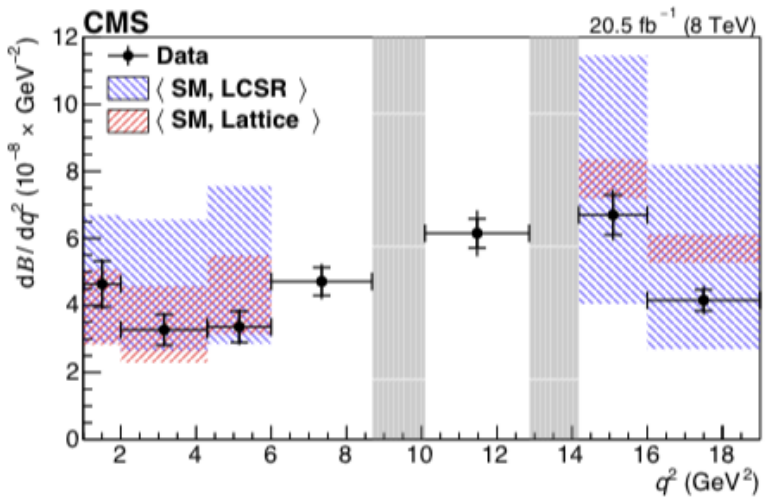

Effect of ΔR(B0s,$\pi\pm$) requirement on the $M^{\Delta}(B^0_s\pi^{\pm})$ distribution

- The D0 Collaboration obtains a significance above five standard deviations for the X(5568) state only when an upper limit on $\Delta R = \sqrt{(\Delta\Phi)^2+(\Delta\eta)^2}$ between B^0_s and $\pi^{\pm}$ imposed ($\Delta R<0.3$)

The D0 Collaboration obtains a significance above five standard deviations for the X(5568) state only when an upper limit on $\Delta R = \sqrt{(\Delta\eta)^2 + (\Delta\phi)^2}$ is imposed, namely, $\Delta R < 0.3$. Here, $\Delta\eta$ and $\Delta\phi$ are the pseudorapidity and azimuthal angle (in radians) differences between the directions of the B^0_s and $\pi^{\pm}$. As shown in Fig. 5, a requirement on this variable significantly changes the $M^{\Delta}(B^0_s\pi^{\pm})$ distribution and can even produce a peaking shape; therefore, it is not used in this analysis.

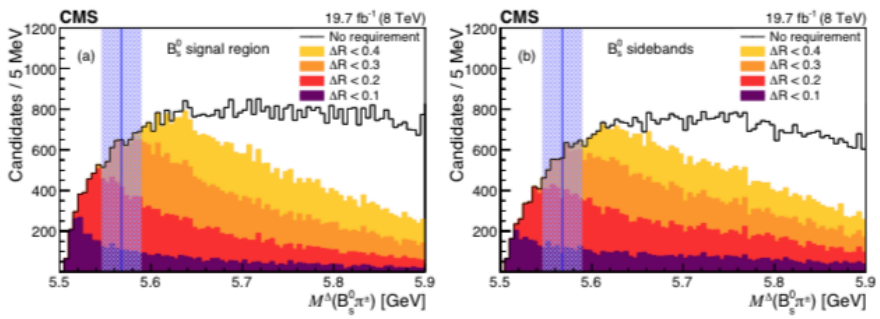

Figure 5: The $M^{\Delta}(B^0_s\pi^{\pm})$ distributions for events in the B^0_s (a) signal and (b) sideband regions for different ΔR requirements. The uncertainties are not shown for the sake of clarity. The vertical band indicates the region $m_X \pm \Gamma_X$.

B_c^+ excited states

CMS: 143 fb^{-1} at 13 TeV data

- Observation of signals consistent with $B_c^+(2S)$ and $B_c^{*+}(2S)$ in the decay channel
  $B_c^+(2S) \rightarrow B_c^+\pi^+\pi^- \rightarrow J/\psi\ \pi^+\pi^+\pi^-$
  $B_c^{(*)+}(2S) \rightarrow B^*_c{}^+\pi^+\pi^- \rightarrow B_c^+(\gamma)\ \pi^+\pi^-$
  $\rightarrow J/\psi\ \pi^+(\gamma)\ \pi^+\pi^-$
- B_c^+ reconstruction: di-muon constrained to J/ψ mass + high purity charged track as π

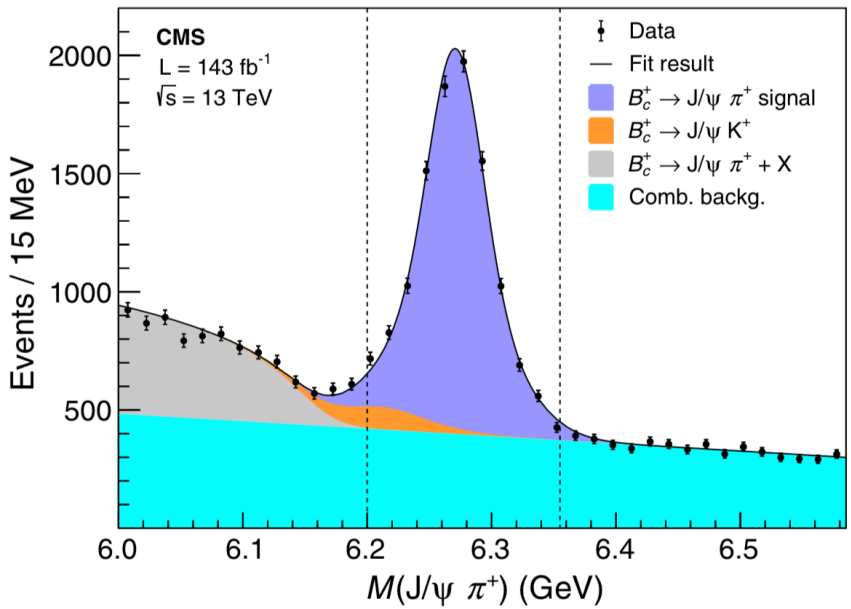

Selection cuts on B_c^+ reconstructed candidates

$$p_T(B_c^+) > 15 \text{ GeV}$$
$$|y^*(B_c^+)| < 2.4$$
$$l(B_c^+) > 100\ \mu m$$
$$\text{Vertex } \chi^2 \text{ prob.} > 10\%$$

B_c^+ signal yield:
$N(B_c^+) = 7629 \pm 226$
$M(B_c^+) = 6271.1 \pm 0.5$ MeV

Phys. Rev. Lett. 122 (2019) 132001

B_c^+ excited states

- $B_c^+(2S)$ and $B_c^{*+}(2S)$ reconstruction: kinematic fit of B_c^+ with 2 oppositely charged particles from the same vertex
- Low energetic γ from $B^*_c \rightarrow B_c^+\gamma$ difficult to detect → $B_c^{*+}(2S)$ peak in the $B_c^+\pi^+\pi^-$ mass spectrum seen at a mass lower than $M(B_c^+(2S))$ → double peak structure

Selection cuts on B_c^+ reconstructed candidates

$$p_T(\pi_1) > 0.8 \text{ GeV}$$
$$p_T(\pi_2) > 0.6 \text{ GeV}$$
$$|y^*(B_c^+\pi^+\pi^-)| < 2.4$$
$$\text{Vertex } \chi^2 \text{ prob.} > 10\%$$

Mass variable defined as (higher resolution):

$$M(B_c^+\,\pi^+\pi^-) - M(B_c^+) + m_{B_c^+}$$

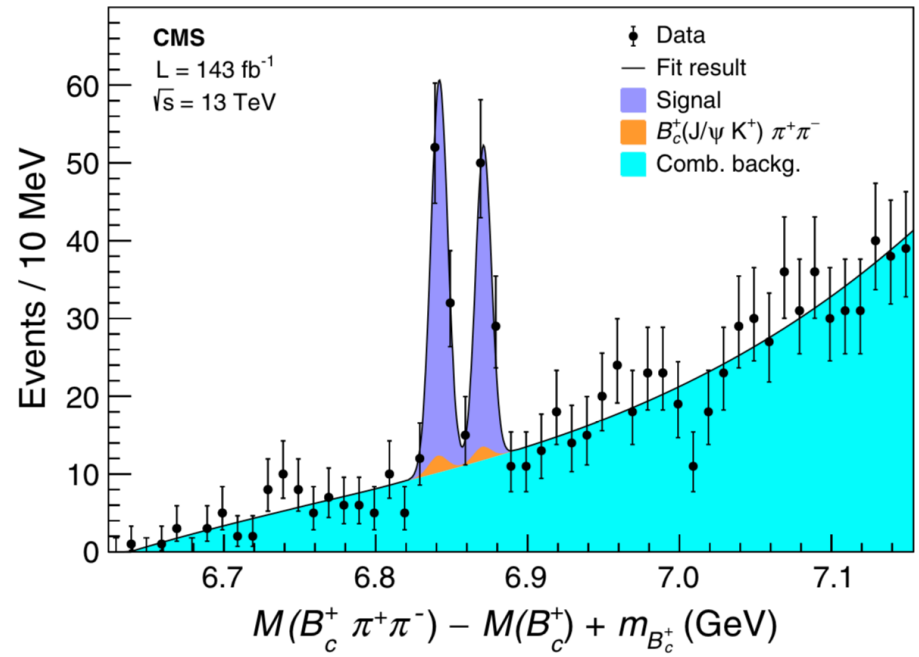

- Good separation of the two states
- $N(B_c^+(2S))=67\pm10$; $N(B_c^{*+}(2S))=51\pm10$; $\Delta M=29.1\pm1.5$ MeV

First measurement of
$M(B_c^+(2S)) = 6871.0\pm1.2(\text{stat})\pm0.8(\text{syst})\pm0.8(B_c^+)$ MeV